



OPEN ACCESS

EDITED BY

Ruth Benavides-Piccione,
Spanish National Research Council (CSIC),
Spain

REVIEWED BY

David A. Leopold,
National Institutes of Health (NIH),
United States
Nina Patzke,
Health and Medical University Potsdam,
Germany

*CORRESPONDENCE

Juliana G. M. Soares
✉ jmsouares@biof.ufrj.br

RECEIVED 01 May 2023

ACCEPTED 16 June 2023

PUBLISHED 05 July 2023

CITATION

Magalhães-Junior EG, Mayer A,
Nascimento-Silva ML, Bonfim V, Lima B,
Gattass R and Soares JGM (2023)
Architecture of the motor and premotor
cortex of the capuchin monkey.
Front. Mamm. Sci. 2:1215424.
doi: 10.3389/fmamm.2023.1215424

COPYRIGHT

© 2023 Magalhães-Junior, Mayer,
Nascimento-Silva, Bonfim, Lima, Gattass and
Soares. This is an open-access article
distributed under the terms of the [Creative Commons Attribution License \(CC BY\)](https://creativecommons.org/licenses/by/4.0/). The
use, distribution or reproduction in other
forums is permitted, provided the original
author(s) and the copyright owner(s) are
credited and that the original publication in
this journal is cited, in accordance with
accepted academic practice. No use,
distribution or reproduction is permitted
which does not comply with these terms.

Architecture of the motor and premotor cortex of the capuchin monkey

Erli G. Magalhães-Junior, Andrei Mayer,
Márcio L. Nascimento-Silva, Vânio Bonfim,
Bruss Lima, Ricardo Gattass and Juliana G. M. Soares*

Laboratory of Cognitive Physiology, Instituto de Biofísica Carlos Chagas Filho, Universidade Federal do Rio de Janeiro, Rio de Janeiro, Brazil

Introduction: Over the last 65 million years, primates have evolved hind- and forelimbs capable of skilled grasping (e.g., tree branches) and manipulation of tools and other objects. The New World capuchin monkey and the Old World macaque monkey stand out among other primates for their manual dexterity. The capuchin monkey is distributed throughout the Amazon and the Atlantic Forests and is the only New World monkey to have evolved an opposable thumb and to have developed the capability of using tools in the wild.

Methods: The present work analyzes the cyto-, myelo- and immunoarchitecture of the motor and premotor areas of the capuchin monkey using Nissl, Gallyas and SMI-32 immunolabeling techniques.

Results: These different staining techniques allowed for the parcellation of Brodmann area 4 into the ventral (F1v), medial (F1m) and dorsal (F1d) areas. Additionally, lateral area 6 was subdivided into the dorsal (F2 and F7) and ventral (F4 and F5) areas. Area F5 was subsequently subdivided into the convexity (F5c), anterior (F5a) and posterior (F5p) areas. Medial area 6 was subdivided into F3 and F6 areas.

Discussion: These motor and premotor areas of the capuchin monkey are similar to those of macaque and humans, and different from those of other New World monkeys. We argue that this is due to differences in manual dexterity across New World monkeys: capuchin monkeys have evolved different types of precision grips, while most of the other New World monkeys exclusively perform whole-hand grips during object manipulation.

KEYWORDS

primates, primary motor cortex, premotor cortex, hand dexterity, capuchin monkey, New World monkeys, RRID: AB_509998

1 Introduction

Skilled hand movements and tool manipulation allow individuals to accurately interact with the external environment in accordance with their needs. The motor areas in the frontal lobe located rostral to the central sulcus (cs) play an important role in these tasks, creating a motor planning and executing the correct sets of movements according to the goal and the available sensory information (Rizzolatti et al., 1997; Rizzolatti et al., 1998; Geyer, 2004; Passarelli et al., 2021).

The primate motor cortex is composed of several specialized areas. Initially, in his classic cytoarchitectonic study, Brodmann (1905) described two regions in the motor cortex: Area 4 (BA4) and Area 6 (BA6). BA4, located in the posterior portion of the precentral cortex, is notable for its giant pyramidal cells (Betz cells) in layer V and for the absence of an inner granular layer. BA4 can be distinguished from BA6 based on the distribution of Betz cells, which are abundant in area 4, and the presence of more dense Layers III and V in BA4. Penfield and Boldrey (1937) confirmed the functional aspect of BA4 showing that electrical stimulation applied to this area elicits movements of specific body parts, indicating the presence of a body map over this region. BA4 was designated primary motor cortex or M1 (also called F1 by Matelli et al., 1985). On the other hand, BA6 was divided in two regions: the supplementary motor area (SMA), located medially, and the premotor cortex (PM), located laterally (Von Economo, 1929; Woolsey et al., 1952; Matelli et al., 1985; Luppino et al., 1991; Matelli et al., 1991).

Further anatomical and physiological studies suggest that M1 (or F1) is actually composed of three architecturally distinct areas located between the anterior margin of the cs and the cortical convexity: the caudal zone (F1c), the intermediate zone (F1i) and the rostral zone (F1r), each of which presents its own cytoarchitecture, neural response properties, connectivity patterns with other cortical areas and its own representation of the contralateral body parts (Strick and Preston, 1978; Stepniewska et al., 1993; Preuss et al., 1996; Preuss et al., 1997).

Subsequent studies in different primates also subdivided PM and SMA into several areas (Vogt and Vogt, 1919; von Bonin and Bailey, 1947; Matelli et al., 1985; Barbas and Pandya, 1987; Matelli et al., 1991; Preuss and Goldman-Rakic, 1991; Watanabe-Sawaguchi et al., 1991; Preuss et al., 1996; Gabernet et al., 1999; Geyer et al., 2000; Belmalih et al., 2009). Cytoarchitectural patterns, cytochrome oxidase staining, and anatomical connections allowed the subdivision of PM in the macaque into four areas: two areas in the dorsal portion of PM (PMd) corresponding to areas F2 (caudal) and F7 (rostral), and two other areas in a ventral portion (PMv) corresponding to areas F4 (caudal) and F5 (rostral) (Matelli et al., 1985; Matelli et al., 1991). PMd and PMv areas play different roles in the control of goal-oriented actions. While PMd is more involved in the planning, selection, and preparation of actions to reach an object, PMv is associated with the planning and control of holding and manipulating objects (Kantak et al., 2012).

SMA was subdivided into two areas: F3 and F6 (Matelli et al., 1985; Matelli et al., 1991). F3 contains a complete representation of body movements, with a prevalence of the proximal arm, leg, and

axial movements. Electrical stimulation in F3 often evokes complex movements, involving the proximal and distal joints of the forelimbs (Luppino et al., 1991; Tanji, 2001). On the other hand, motor responses in F6 can be evoked only with comparatively higher electric currents, typically eliciting complex arm movements (Luppino et al., 1991). The activity of F6 neurons during the performance of movement sequences shows that this area is preferentially active during the learning of new sequences and during the initial phase of the performance. It is believed that F6 is involved in controlling new movements, while F3 controls movements that have already been learnt (Rizzolatti et al., 1990; Matsuzaka et al., 1992).

Motor and somatosensory areas interact in order to control manual behavior in primates. The ability to perform skillful hand movements and to manipulate objects are milestones in primate evolution. The ability to grasp and to manipulate objects varies among clades of primates. It depends on both the anatomical organization and on the functional constraints that subserve forelimb movement and action planning (Truppa et al., 2019). While Old World primates can perform precision manual movements, most New World primates perform manual movements using the whole hand when grasping objects, without the fine coordination of their digits (Fragaszy, 1983). This difference seems to be related to the fact that the primary motor cortex (M1), as well as PM and SMA of Old World primates, have distinct and more specialized subdivisions than those observed in New World primates (Wu et al., 2000; Kaas, 2012).

Here, we investigated the architecture of motor cortical areas in the capuchin monkey (*Sapajus apella*), a New World monkey with brain organization, sulcal pattern and localization of cortical areas similar to the macaque (Gattass et al., 1987; Fiorani et al., 1989; Rosa et al., 1993; Padberg et al., 2007; Reser et al., 2014; Mayer et al., 2016). Unlike other New World monkeys, the capuchin monkey can perform 16 different types of precision prehension, including thumb and index finger opposition and the use of tools (Moura and Lee, 2004; Spinozzi et al., 2004; Mannu and Ottoni, 2009). Therefore, describing the fine cytoarchitecture of the motor areas in the capuchin monkey allows us to infer homologies between the brain regions of New and Old World monkeys. This may help us to understand how these structures evolved and how they reached their current level of organization and complexity.

2 Materials and methods

Seven capuchin monkeys (*Sapajus* spp., formerly classified as *Cebus* spp.) were used in this study. All subjects were adults (4 males and 3 females) weighing between 2.1 and 4.4 kg. These same individuals were also used in other unrelated anatomical studies. All experimental procedures were approved by the Ethics Committee for the Care and Use of Experimental Animals (CEUA-CCS protocol # IBCCF-119 and 190-06/16, at the Center for Health Science, Federal University of Rio de Janeiro). Our procedures were also in accordance with the guidelines of the National Institute of Health for the Care and Use of Laboratory Animals (NIH-USA).

The animals were euthanized with a lethal dose of sodium pentobarbital (40mg/kg) administered intravenously. After reaching deep anesthesia, they were transcardially perfused with 0.9% saline, followed by 4% paraformaldehyde in phosphate buffer, 4% paraformaldehyde in 2.5% sucrose phosphate buffer, 4% paraformaldehyde in 5% sucrose phosphate buffer and, finally, in 10% sucrose phosphate. After perfusion, the brain was removed from the skull and post-fixed with 4% paraformaldehyde in 30% sucrose for approximately 24 hours. After this post-fixation period, the brain was sectioned on a cryostat at 40 or 50 μm thickness, in the parasagittal (5 animals) or coronal (2 animals) plane.

2.1 Histological processing

Alternate sections were stained for cell bodies (Nissl method), myelinated fibers (Gallyas, 1979), or for neurofilaments M and H of pyramidal neurons (immunohistochemistry with SMI-32 monoclonal antibody) (Sternberger and Sternberger, 1983; Campbell and Morrison, 1989; Hof and Morrison, 1995). For SMI-32 immunohistochemistry, individual free-floating sections were placed in separate wells and washed three times with 0.1 M saline phosphate buffer (PBS) for 10 minutes. Subsequently, the slices were incubated with 2% bovine serum albumin (BSA) in a solution of 0.3% triton X-100 in PBS (PBS-Tx) for 1h. After three washes in PBS, sections were kept under gentle agitation overnight at room temperature in a solution containing the mouse monoclonal SMI-32 antibody (1:5000 dilution, Covance Research Products Inc. Cat# SMI 32R-500, RRID: AB_509998) in 2% BSA and 0.3% PBS-Tx. The sections were washed three times in PBS, incubated with biotinylated anti-mouse secondary antibody (1:200 dilution, Vector Laboratories) for 2h. Subsequently, they were washed with PBS (3 times for 10 minutes) and incubated for 1h in avidin-biotin complex ABC (1:500 dilution, Vectastain Elite, Vector Laboratories). Immunoreactivity was revealed with a 0.05% solution of 3,3'-diaminobenzidine (DAB) and 0.1% solution of nickel ammonium sulfate. The sections were then mounted on bi-gelatinized slides, dehydrated in solutions containing increasing concentrations of alcohol (75%, 90%, 100%, and again 100%, 1 min in each of the solutions), clarified with xylene (twice for 3 min) and coverslipped with di-n-butylphthalatexylene (DPX).

2.2 Data analysis

The histological sections were photomicrographed using a Zeiss Axioplan-2 microscope equipped with a digital color camera (1600 3 1200, 3/4" chip, 36 bits, MBF) and a motorized stage (Mac5000 LUDL) controlled by the Neurolucida software (MBF Biosciences, INC. Williston, VT, USA), running on a Dell workstation. The images of the entire histological sections were produced by the Virtual Tissue 2D module. Before the acquisition, in order to reduce possible background noise, the images were corrected for color balance, brightness, and contrast, in the acquisition system itself. Images were captured with a 5x, 10x and 40x objective.

The photomicrographs were analyzed on a computer screen using the Canvas graphic software (Canvas X 2016/2017/2018,

ACD Systems, USA). Different magnifications were used to establish the anatomical borders between different areas and subareas of the motor cortices. Cytoarchitectural characteristics were compared in the same or across sections. For the SMI-32 analysis, the evaluated characteristics were size, density and laminar distribution of immunostained cell bodies. Additionally, we evaluated the extent and the thickness of apical dendrites and the staining intensity of reactive neuropils across cortical layers. In myelin-stained sections, we evaluated the density, orientation, and laminar distribution of the stained axons, as well as fiber thickness. In Nissl-stained sections, we evaluated the size, distribution, and density of neuronal cell bodies across cortical layers. The differences in the relative thickness of cortical layers were another criterion used to identify the borders between areas and, when the case, enable further subdivisions of a particular area. Borders between areas were established only after common agreement among at least three independent investigators in our team. After the cytoarchitecture analysis, cortical layer IV depicted in Nissl sections of case R13-01 (left hemisphere) was delimited in the photomicrographs using the Neurolucida software. Subsequently, we used the CARET software (Van Essen et al., 2001; Van Essen, 2005; Kalwani et al., 2009; Zhong et al., 2010; Bezgin et al., 2012; Van Essen, 2012; Van Essen, 2012; Chaplin et al., 2013) to align the sections and obtain a three-dimensional (3D) reconstruction of the motor cortex with its corresponding cortical areas.

3 Results

Here, we characterized the architectural subdivisions of the motor and premotor cortex in the capuchin monkey. We analyzed both hemispheres of male and female subjects and did not find any significant anatomical difference between left vs. right hemispheres or between the sexes. Within this region, which extends from the upper margin of the central sulcus (cs) to the rostral tip of the superior arcuate sulcus (sas) and the fundus of the inferior arcuate sulcus (ias), we characterized nine architectonic areas: F1, F2, F3, F4, F5c, F5p, F5a, F6 and F7 (Figure 1, Table 1). Considering the cortical similarities observed between macaque and capuchin monkeys, each area was designated by a terminology similar to the one adopted in previous studies in Old World monkeys (Matelli et al., 1985; Matelli et al., 1991; Geyer et al., 2000; Belmalih et al., 2009).

Area F1 extends along the entire upper bank of cs, bordering area 3a, caudally, and areas F2 and F4, rostrally (Figure 1). Area F2 is localized dorsally, in the caudal portion of the premotor cortex and extends from the caudal tip of sas to the region where sas fuses with ias. Rostral to F2 we found area F7, which extends to the rostral tip of sas, bordering prefrontal area 9 (not shown). Medial to areas F2 and F7, starting at the dorsal edge of the hemisphere and extending to its medial surface, we found areas F3 and F6 (not shown in Figure 1).

Ventral to sas, we found areas F4 and F5. Area F4 was located more caudally, extending from the rostral border of F1 to the caudal borders of F5c and F5p. The F5a subdivision was located entirely inside the posterior bank of ias, close to its inferior tip. The F5c

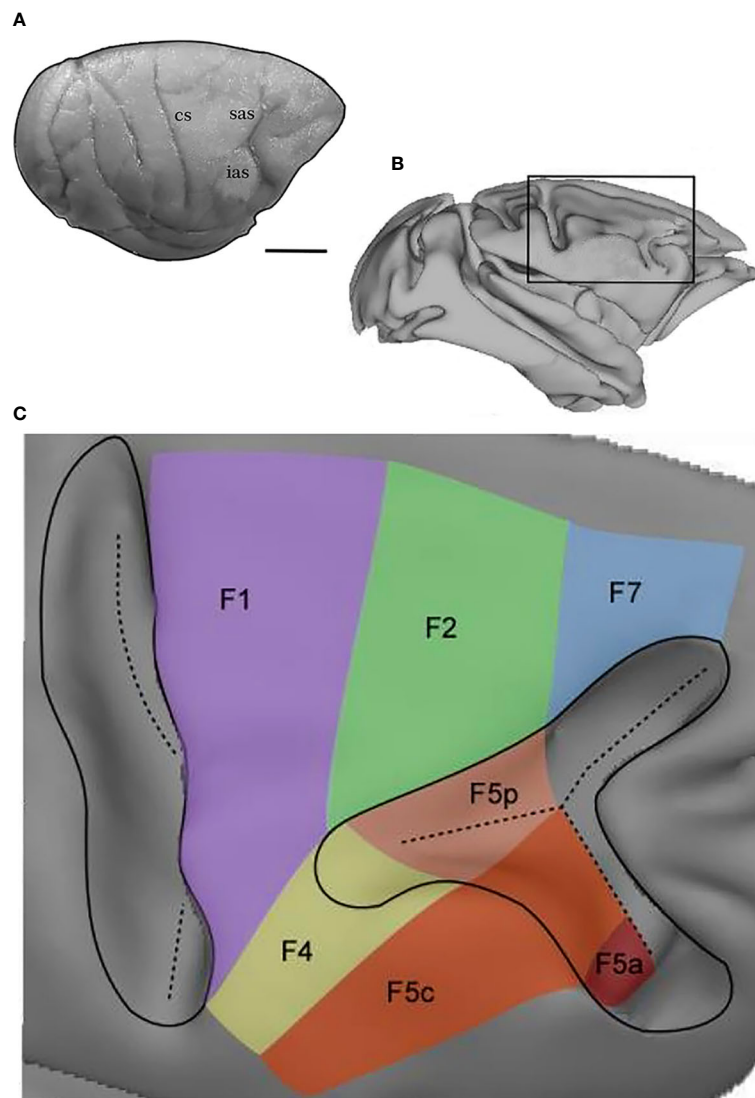


FIGURE 1

Architectonic subdivisions of the capuchin monkey motor and premotor cortices. **(A)** Photograph showing a lateral view of the left hemisphere of a typical capuchin brain. **(B)** 3D reconstruction of the hemisphere shown in **(A)** based on cortical layer IV, which allows for an in-depth view of the cortical tissue buried inside the sulci. The black rectangle delimits the region of interest containing the motor and premotor cortices, magnified in the 3D reconstruction shown in **(C)**. The different colors represent the areal subdivisions defined by our present work. The solid lines represent the outline of the central and arcuate sulci. The dashed lines represent the fundus of the sulci. Abbreviations: cs, central sulcus; sas, superior arcuate sulcus; ias, inferior arcuate sulcus. Scale bar **(A, B)**: 1 cm.

subdivision was located dorsal to F5a and extends from the fundus of ias to the ventral convexity of the premotor cortex, ventrally to area F4 (Figure 1). The F5p subdivision was located at the fundus of the spur.

3.1 Architectural characterization of the primary motor cortex (M1 or F1)

Area 4 (F1) and area 6 (F2, F3, F4, F5, F6 and F7) are characterized by the absence of layer IV and are thereby designated as agranular cortex. The borders between these areas were conspicuous using all three staining methods: SMI-32, Nissl and myelin (Figures 2–4). In both SMI-32 and Nissl, we observe a

conspicuous area F1 with a large number of pyramidal cells and many giant cell bodies (Betz cells) lined up in layer V. This pattern changed almost abruptly from area F1 to areas F2, F4 and F3, where we clearly observed a thinner layer V with a smaller density of giant cells (Figures 2, 3). Layer III was also thicker in area F1 compared to all others frontal areas, with cell bodies arranged in columns. Myelin staining revealed a high degree of myelination in all areas, with areas F2–F7 showing a greater organization of the vertical bundles of fibers (Figures 4, 5).

As can be observed in SMI-32-immunoreacted sections (Figures 2, 6), area F1 was characterized by a thick layer 3 with a moderate density of medium-sized pyramidal cell bodies and thin apical dendrites (Figure 6). The infragranular layers exhibited a low density of neurons, consisting of medium to large-sized pyramidal

TABLE 1 Areal subdivision criteria.

Subdivision criteria/Areas	F1c	F1i	F1r	F2v	F2d	F7
Layer IV	–	–	–	–	–	–
Density of Betz cells	+++	+	++	–	–	–
Betz cells arrangement	Multiple rows	Single row	Multiple to single row	–	–	–
Layer V density of pyramidal cells	+++	+	++	+	++	+
Layer III thickness	+++	+++	++	+	++	++
Layer III density of pyramidal cells	++	+	++	+++	++	++
Myelination pattern	Less myelinated than neighboring areas 3a, F2 and F4			Denser than adjacent areas		Trilaminar
Organization of the fibers	Homogeneous			Homogeneous		Radial fibers
Subdivision criteria/Areas	F4	F5p	F5c	F5a	F6	F3
Layer IV	–	–	–	+	–	–
Density of Betz cells	–	–	–	–	–	–
Betz cells arrangement	–	–	–	–	–	–
Layer V density of pyramidal cells	+	++	++	+	+	+
Layer III thickness	++	++	++	+	++	+
Layer III density of pyramidal cells	++	++	++	+	++	+
Myelination pattern	More myelinated than F1	Trilaminar	Trilaminar	Trilaminar		
Organization of the fibers	Smooth inner Baillarger band	Radial fibers	Radial plexus	Widely distributed		

cell bodies in layer V and low density of neuropils in layer VI. Compared to the immediately neighboring 3a, F4, and F2 areas, area F1 showed a greater neuronal density than the former areas, especially in layer III and particularly in layer V, which clearly showed a higher density of Betz cells arranged in multiple rows.

In Nissl-stained sections (Figures 3, 7), F1 showed a relatively poor lamination compared to parietal and other frontal areas. Layers III and V were relatively prominent, where layer IIIb presented smaller cell bodies in higher density than observed in layer IIIa. Layer Va was densely populated by cell bodies of small size, while layer Vb contained medium–large cell bodies and Betz cells. Layer VI was thick, but did not show a clear border with layer Vb. The presence of Betz cells in layer Vb was the best criterion to differentiate area F1 from its neighboring areas 3a, F2 and F4, since the cell bodies in these later areas are smaller than the Betz cells.

Area F1 was slightly less myelinated than neighboring areas 3a, F2, and F4 (Figures 4, 5). Layer VI and the lower portion of layer V exhibited intense myelination, while the upper portion was mildly less myelinated with a pale inner band of Baillarger.

Area F1 could be further subdivided into caudal (F1c), intermediary (F1i), rostral (F1r) (Figures 2, 3) and medial (F1m) (Figure 8) portions based on the density of Betz cells in layer V (Figure 7) and on the cell density and thickness of layer III. Area F1c showed a thicker layer III with medium-to-small-sized pyramidal cells organized in multiple rows in the lower portion of the layer and projections of thin apical dendrites leading to the upper layers. Layer V of F1c exhibited multiple rows of large-sized pyramidal cell bodies. Layer III of F1i was thinner than in F1c and the pyramidal cells of layer V were sparse and tended to form a single row. In F1r,

layer III was thinner and more intensely immunolabeled than in the other subdivisions of F1. In coronal sections (Figure 8), we observed that layer III of F1m was thinner and that the pyramidal cells in layer V were smaller than those in the lateral portions.

3.2 Architectural characterization of the premotor cortex

We identified four areas within the premotor cortex. Initially, we will describe the areas located in its dorsal portion (F2 and F7) and subsequently the areas located in its ventral portion (F4 and F5).

3.2.1 Area F2

Area F2 (Figures 2, 6) was characterized by a comparatively thin layer III with medium-to-small-sized pyramidal cell bodies located mainly in its lower portion, by bundles of apical fibers distributed vertically, and by bundles of basal fibers distributed horizontally. Layer V was characterized by the presence of medium-to-large cell bodies, spaced apart in a single row (Figure 6). Compared to neighbouring areas F1 and F7, area F2 presented smaller cell bodies than in F1 but larger cell bodies than in F7. In Nissl-stained sections, area F2 exhibited a layer II composed of densely packed small cell bodies and layers III, V and VI that could be clearly further subdivided. Layer IIIb was denser, with cell bodies larger than those in layer IIIa; Layer Va was less dense than layer Vb, showing larger cell bodies arranged in rows. Layer Vb exhibited a sharp limit with layer VIa, which was populated by relatively small

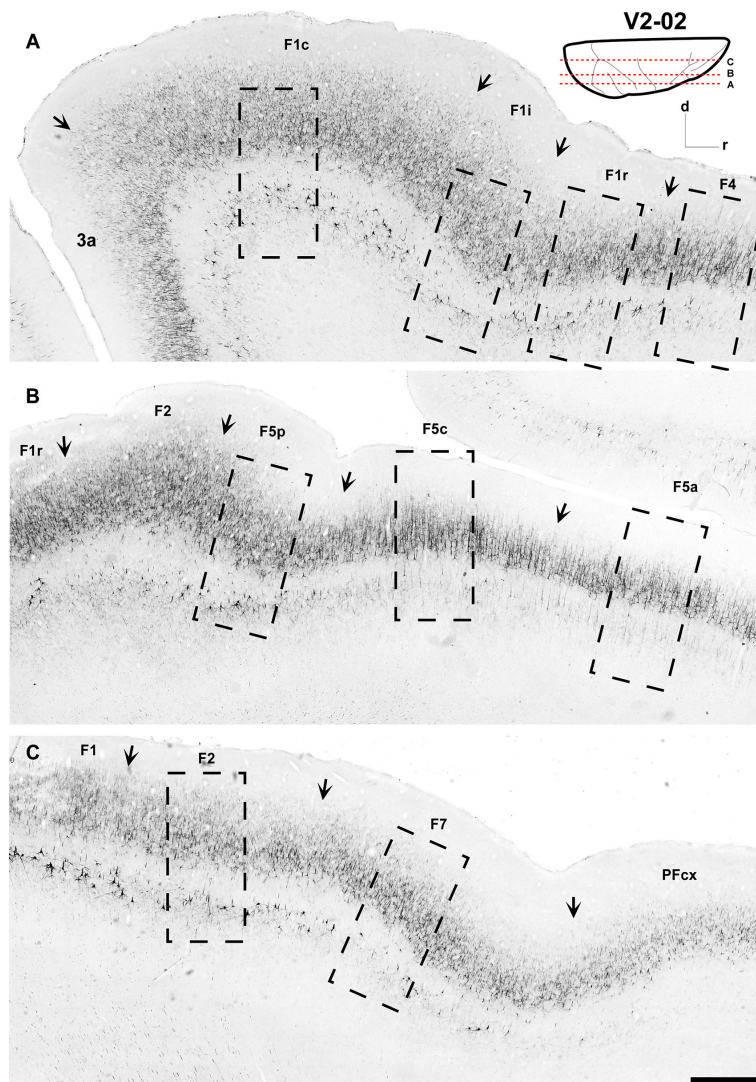


FIGURE 2

Low-power photomicrographs of three SMI-32-immunostained, parasagittal sections containing motor and premotor cortical areas of Case V2-02. (A–C) Sections, from lateral (A) to medial (C) levels as indicated in the insert at the top right. Arrows indicate the borders between areas. A magnified view of the cortical region depicted inside the dashed-lined rectangles are shown in Figure 6. Scale bar: 1 cm.

cell bodies. Layer VIa was less densely packed than layer Vb but more densely packed than layer VIb (Figure 7). Area F2 showed a denser myelination than adjacent areas. It was possible to identify a smooth inner band of Baillarger and the distribution of radially organized dense myelinated fibers (Figures 4, 5).

Area F2 could be further subdivided into dorsal (F2d), and ventral (F2v) portions based on layer III immunoreactivity and layer V cell density, especially in coronal sections (Figures 8C, D). Area F2v differed from F2d by a lower density of pyramidal cells in layers III and V (Figure 9B). SMI-32-immunoreactivity in layer III of F2v was weaker than in F2d and the pyramidal cells were smaller and sparser (Figure 9A).

3.2.2 Area F7

In SMI-32-immunostained sections (Figures 2, 6), area F7 was identified by a thin, low-density layer III with small pyramidal cell

bodies clustered in its lower portion and long apical dendrites organized in its upper portion (Figure 6). Layer V presented only scattered medium-sized pyramidal cell bodies.

In Nissl-stained sections (Figures 3, 7), area F7 exhibited a sublamination of layer III, with layer IIIb showing larger, well stained, and more spaced out cell bodies than layer IIIa. Layer V was relatively thin, with homogeneously distributed small cell bodies and a few medium-sized cell bodies clustered near the centre of the layer. Area F7 myelination pattern revealed a tri-laminar structure, with an inner band of Baillarger and radial myelinated fibers slightly denser than in area F2 (Figure 4).

3.2.3 Area F4

Area F4 was characterized by a layer III that was thinner than in F1 (Figures 2, 6) and contained an intermediate density of medium-to-small-sized pyramidal cell bodies with thin apical dendrites

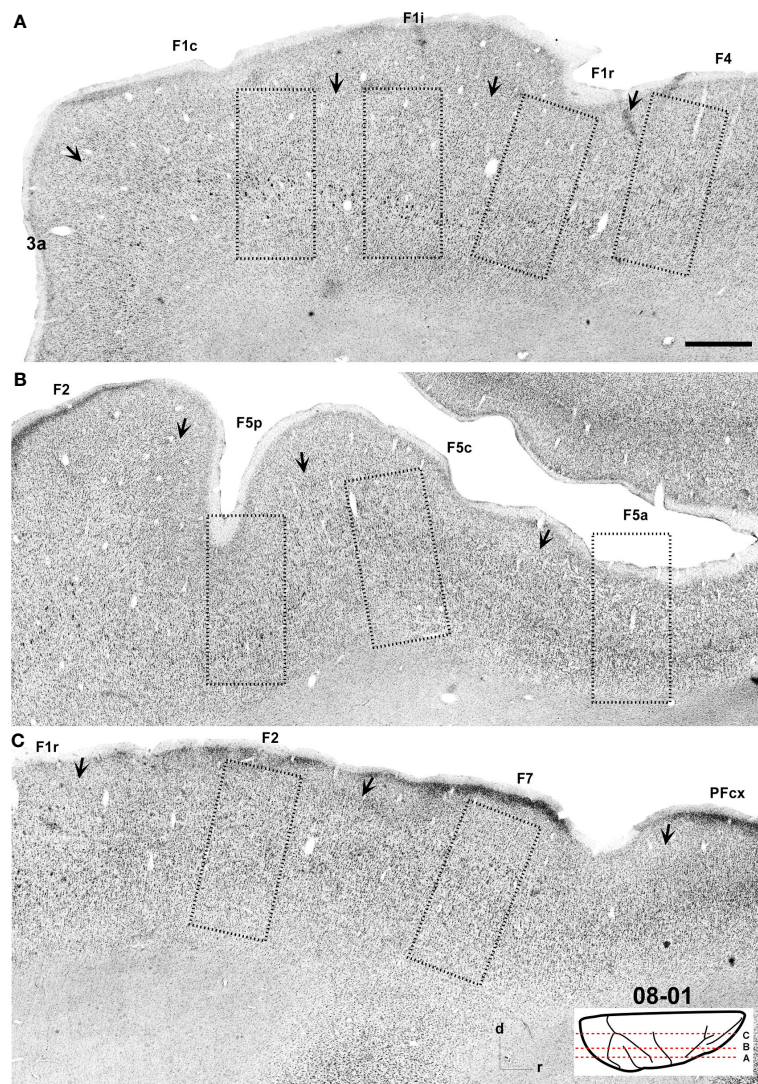


FIGURE 3

Low-power photomicrographs of Nissl-stained, parasagittal sections containing motor and premotor cortical areas of Case 08-01. (A–C) Sections from lateral (A) to medial (C) levels as indicated in the insert at the bottom right of the figure. Arrows indicate the borders between areas. A magnified view of the cortical region depicted inside the dashed-lined rectangles are shown in Figure 7. Scale bar: 1 cm.

directed towards the upper region of the layer (Figure 6). Layer V was distinguished by a lower density of medium-to-large-sized pyramidal cell bodies organized in a single row. Compared to adjacent areas F1 and F5, layer III in F4 showed a lower density of pyramidal cell bodies than F1 and was thicker than in F5 (Figures 6, 7).

In Nissl-stained sections (Figures 3, 7), area F4 revealed a well-developed and laminated layers III and V, with cells well organized in columns. Layer IIIa exhibited a dense packing of small cell bodies, while layer IIIb showed larger cell bodies that were more widely spaced. Layer Va was similar to layer IIIb, but showed greater cell density, while layer Vb exhibited medium-to-large cell bodies, organized in single rows and more widely spaced. In myelin-stained sections, area F4 was more myelinated than F1 and showed a smooth inner band of Baillarger, evidencing the heterogeneity of layer V (Figures 4, 5).

3.2.4 Area F5

Area F5 occupies the rostral portion of PMv and was further subdivided into areas F5p, F5c and F5a. In SMI-32-immunostained sections, area F5p was characterized by a thin layer III (Figures 2, 6) with a medium density of small pyramidal cells with thin basal dendrites and apical dendrites projecting towards the upper portion of the layer (Figure 6). Layer V was distinguished by a low density of medium-to-small-sized pyramidal cell bodies. Different from adjacent area F5c, layer V in F5p did not show any sub-lamination in Nissl-stained sections (Figures 3, 7). Additionally, it contained medium-to-large-sized pyramidal cell bodies arranged in a single row.

In myelin-stained sections, area F5p exhibited a lighter bilaminar appearance than in F4, with a slightly thicker and denser inner band of Baillarger. The myelinated fibers were denser and distributed radially along the rostro-caudal axis of the lower layers (Figures 4, 5).

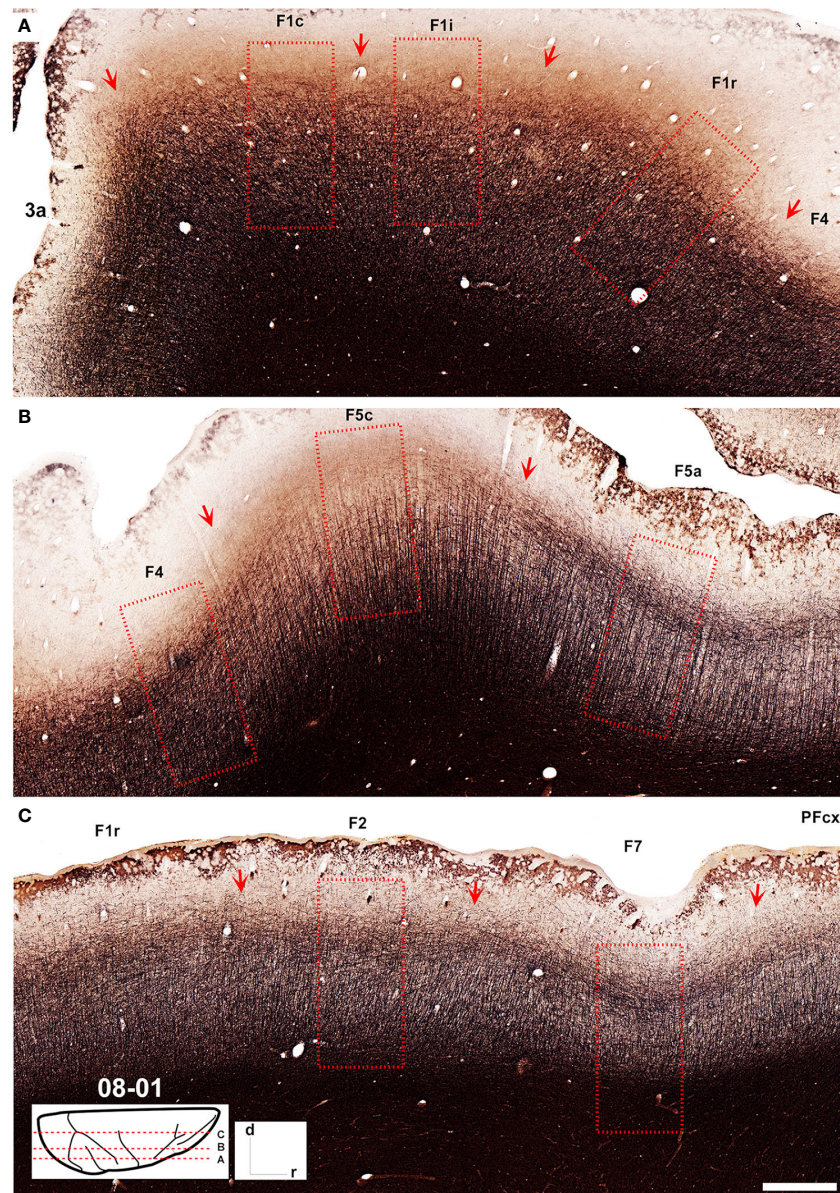


FIGURE 4

Low-power photomicrographs of Gallyas-stained, parasagittal sections containing motor and premotor cortical areas of Case 08-01. (A–C) Sections from lateral (A) to medial (C) levels as indicated in the insert at the bottom left of the figure. Arrows indicate the borders between areas. A magnified view of the cortical region depicted inside the dashed-lined rectangles are shown in Figure 5. Scale bar: 1 cm.

In SMI-32-immunostained sections, area F5c was identified by a thin layer III containing a relatively low density of pyramidal cell bodies, a layer V with densely packed medium-to-small-sized pyramidal cell bodies exhibiting radially organized bundles of apical fibers, and a layer VI with a low neuropil density. Compared to neighbouring areas F5p and F5a, area F5c showed a lower density of cell bodies, especially in layer III, and a higher density of small-to-medium-sized pyramidal cell bodies in layer V (Figures 2, 6).

In Nissl-stained sections, area F5c exhibited a denser layer II and a sub-lamination of layers III and V. Layer IIIa was thinner, with smaller and homogeneously distributed cell bodies, while layer IIIb had larger and more densely packed cell bodies. Sublayer Va

presented medium sized, spaced out cell bodies. Layer Vb presented larger and spaced out cell bodies and exhibited a smooth transition with layer VI, which presented small cell bodies organized in columns (Figures 3, 7).

In myelin-stained sections, area F5c revealed a smooth inner band of Baillarger and a clear distribution of thin and vertically oriented myelinated fibers. Its lower portion was denser than its upper portion, and the myelinated fibers were distributed in a clear radial plexus with fibers arranged further apart. This trilaminar appearance and the arrangement of myelinated fibers were the two best criteria to identify area F5c (Figures 4, 5).

In SMI-32-immunostained sections, area F5a was characterized by a lower density of pyramidal cell bodies in layers III and V

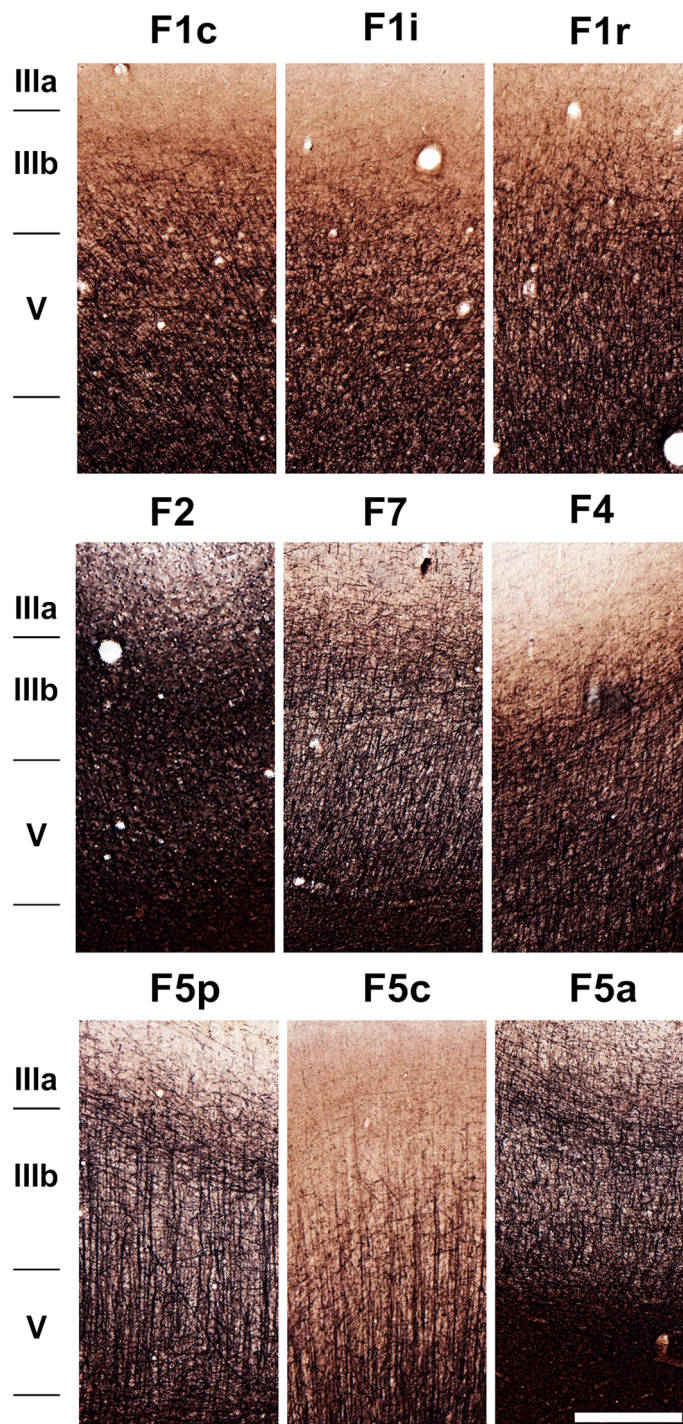


FIGURE 5

Photomicrographs showing the architecture of areas F1c, F1i, F1r, F2, F7, F4, F5p, F5c, and F5a as revealed by Gallyas staining. The sections correspond to the dashed rectangles depicted in Figure 4. Scale bar: 1 mm.

compared to neighbouring areas F5c and the prefrontal cortex. Layer V presented rare small-sized pyramidal cell bodies, and layer III exhibited small pyramidal cell bodies in its lower portion and short apical bundles of fibers directed toward the pial surface (Figures 2, 6).

In Nissl-stained sections, area F5a exhibited a prominent layer IV and a sub-lamination of layers III and VI. The presence of layer

IV was the main criteria to differentiate F5a from neighbouring area F5c, and its lower cell density was the best criteria to identify the border between F5a and the prefrontal cortex. Layer III of F5a was relatively thin and layer IIIa showed higher density of cells compared to layer IIIb. Layer V was also thin, formed by small cell bodies, and its boundary with layer VIa was difficult to establish, except for the fact that layer VIa was less dense than layer V, but

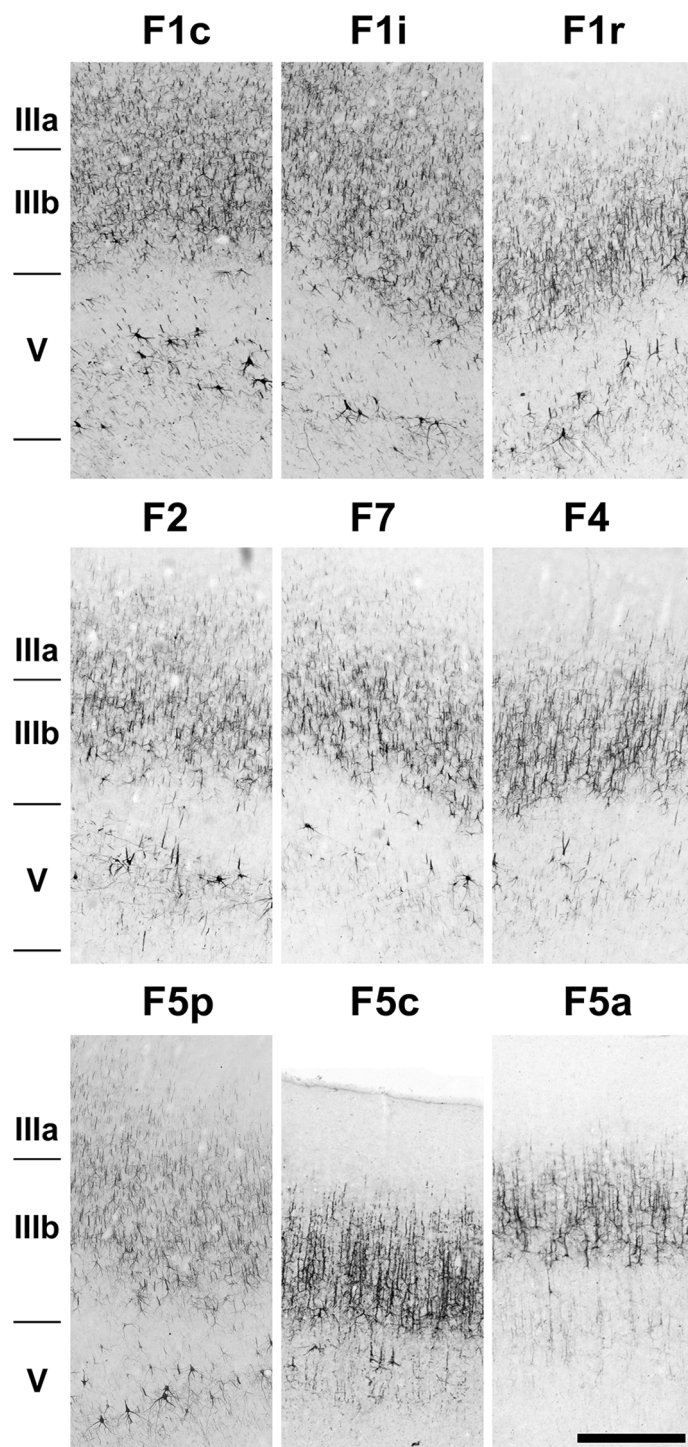


FIGURE 6

Photomicrographs showing the architecture of areas F1c, F1i, F1r, F2, F7, F4, F5p, F5c, and F5a as revealed by SMI-32 immunostaining. The sections correspond to the dashed rectangles depicted in Figure 2. Scale bar: 1 mm.

denser than layer VIb. Layer IV was thin, with small cell bodies, smaller than those of the other layers (Figures 3, 7).

Similar to area F5c, area F5a presented a tri-laminar pattern, with high myelination in its lower portion, an intermediate portion formed by thin myelinated fibers more widely distributed and an upper portion showing a denser inner band of Baillarger compared to F5c (Figures 4, 5).

3.3 Architectural characterization of the supplementary motor areas

3.3.1 Area F6

Area F6 was characterized by the highest density of cell bodies, as revealed by both Nissl and SMI-32 staining (Figures 8A, B). Layer III was relatively thick, composed of densely packed small cell

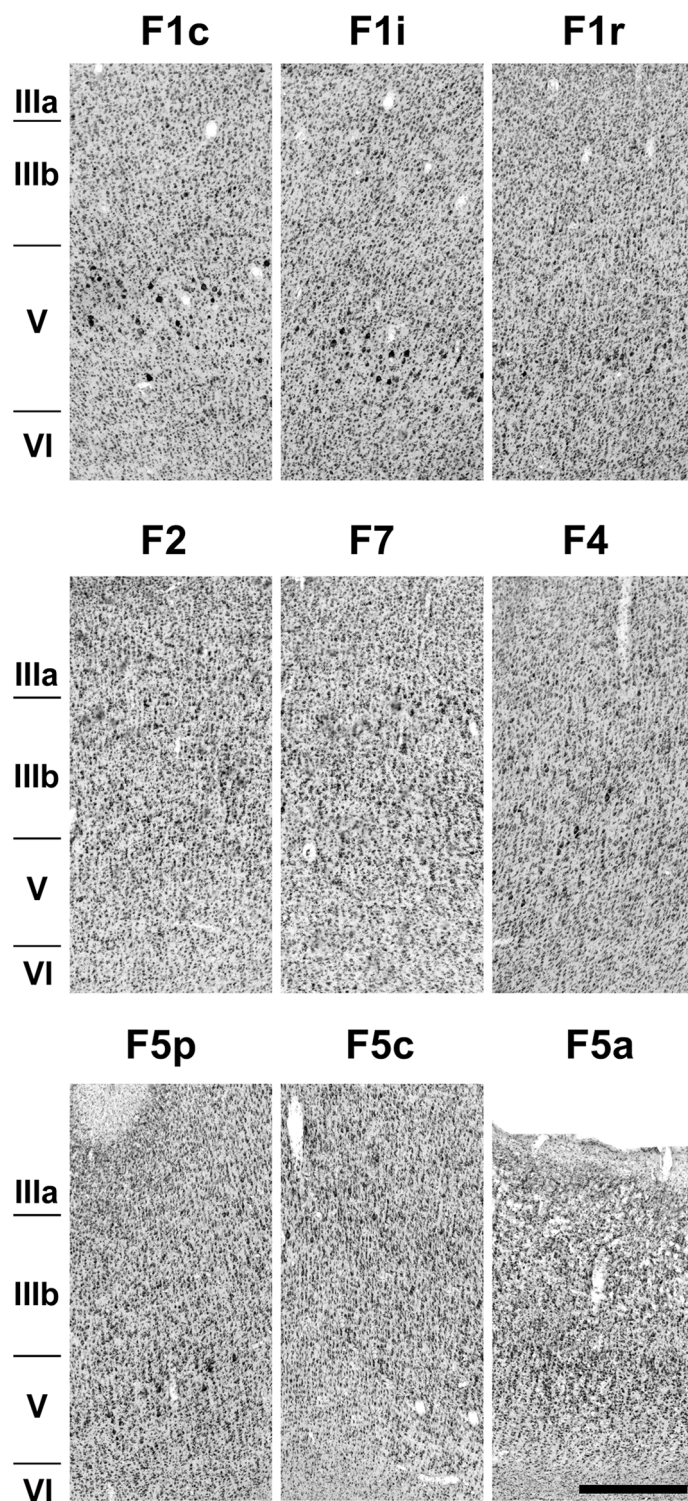


FIGURE 7

Photomicrographs showing the architecture of areas F1c, F1i, F1r, F2, F7, F4, F5p, F5c, and F5a as revealed by Nissl staining. The sections correspond to the dashed rectangles depicted in Figure 3. Scale bar: 1 mm.

bodies in its lower portion, and thick apical dendrites extending to its upper portion. Layer V was also relatively thick and contained smaller pyramidal cell bodies than in layer III, which were spaced apart in multiple rows and exhibited thin apical dendrites projecting towards the upper layers (Figure 9A).

In Nissl-stained sections (Figure 9B) area F6 showed a barely discernible layer II, a layer III subdivided into a less dense sublayer IIIa, with small, compacted and homogeneously spread-out cell bodies. Layer IIIb was denser, showing larger and more sparse cell bodies than in layer V. Layer VI was paler and showed smaller radially arranged cell bodies.

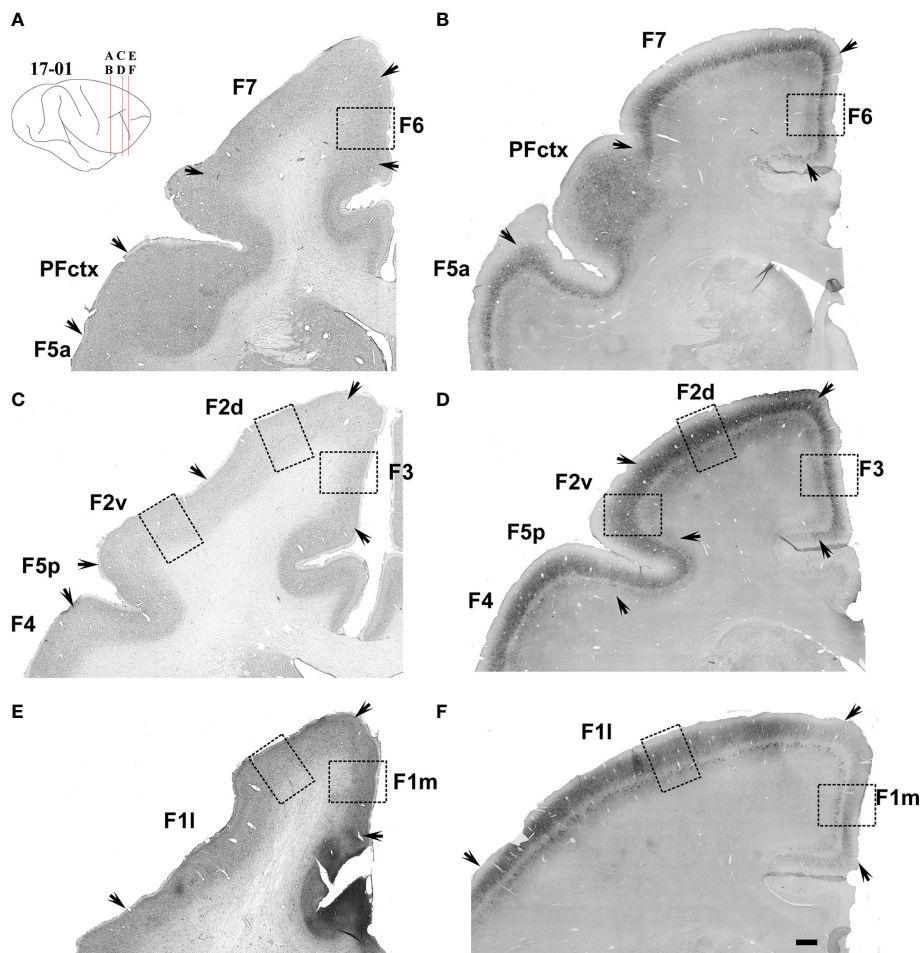


FIGURE 8

Low-power photomicrographs of Nissl-stained (left column, Case 11-08), and SMI-32-immunostained (right column, Case 17-01) coronal sections containing the motor and premotor cortical areas located between sas and cs. (A–F) Sections from posterior (A, B) to anterior (E, F) levels as indicated in the insert at the top left of the figure. Arrows indicate the border between areas. A magnified view of the cortical region depicted inside the dashed-lined rectangles are shown in Figure 9. Scale bar: 1 cm.

3.3.2 Area F3

Area F3 was characterized by thinner and less dense layers III and V (Figure 8D). Layer III presented spaced out small-sized cell bodies, with thinner and more prevalent apical dendrite extensions. Layer V presented few pyramidal cells, which are grouped separately (Figure 9A).

In Nissl-stained sections (Figures 8C, 9B), area F3 was characterized by a thin layer with radial organization. Layer II was barely discernible, and layer III was thinner and slightly denser in its lower portion. Layer V presented scattered groups of medium-sized cell bodies. Layer VI was thicker, organized radially and contained small cell bodies.

4 Discussion

The aim of the present study was to characterize the anatomical organization of the motor and premotor areas in the capuchin monkey. In total, seven animals were studied, including females and males' subjects of different body weights and sizes. Using Nissl,

Gallyas and SMI-32 immunolabeling techniques, we were able to subdivide Brodmann area 4 into ventral (F1v), medial (F1m) and dorsal (F1d) areas. Additionally, we subdivided lateral Brodmann area 6 into dorsal (F2 and F7) and ventral (F4 and F5) areas. Area F5 was subsequently subdivided into the convexity (F5c), anterior (F5a) and posterior (F5p) areas. Finally, medial Brodmann area 6 was subdivided into F3 and F6.

Brodman (1905) described the cytoarchitectonic areas 4 and 6 as unique and single cortical regions. However, subsequent works using techniques such as histochemical and immunocytochemical staining, connectivity patterns and neuronal response properties enabled further subdivisions of these two original areas (Campbell, 1904; Vogt and Vogt, 1919; von Bonin and Bailey, 1947; Matelli et al., 1985; Barbas and Pandya, 1987; Barbas and Pandya, 1989; Matelli et al., 1991; Preuss and Goldman-Rakic, 1991; Watanabe-Sawaguchi et al., 1991; Stepniewska et al., 1993; Preuss et al., 1996; Preuss et al., 1997; Rizzolatti et al., 1998; Gabernet et al., 1999; Geyer et al., 2000; Luppino and Rizzolatti, 2000; Rizzolatti and Luppino, 2001; Belmalih et al., 2009; Caminiti et al., 2015; Caminiti et al., 2017; Kurata, 2018). The primate cortical areas expanded substantially since their last common ancestor (Goldring and

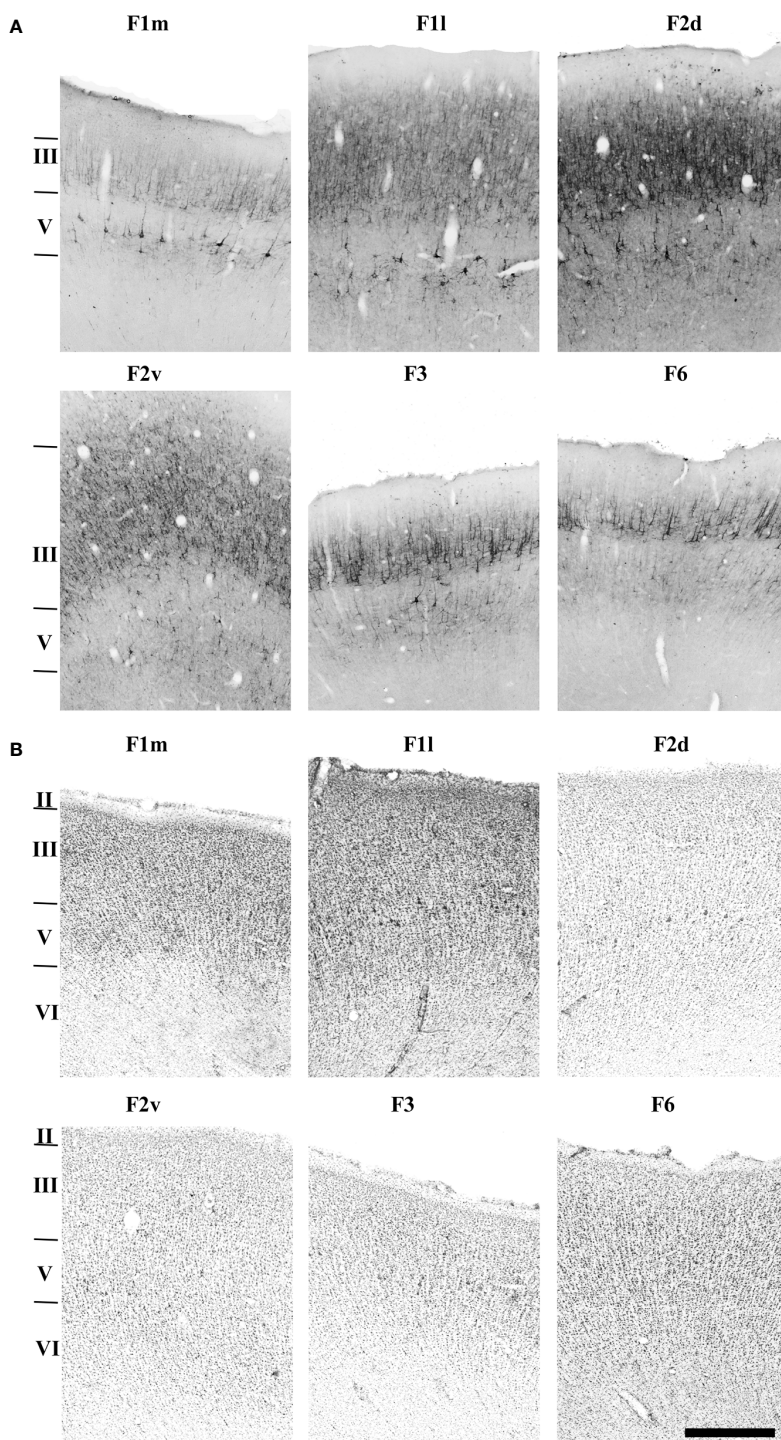


FIGURE 9

Photomicrographs showing the architecture of areas F1m, F1l, F2d, F2v, F3 and F6 revealed by SMI-32 immunohistochemistry (A), and Nissl staining (B). The sections correspond to the dashed rectangles depicted in Figure 8. Scale bar: 1 cm.

Krubitzer, 2017). This led both to a diversification of the original cortical areas and to the emergence of new areas. In terms of the motor system, this probably led to more elaborate action planning and motor control. Capuchin monkeys are unique New World primates that show great manual dexterity and can thereby shed light into the evolution of primate motor behavior. However, the organization of its motor and premotor cortices is still poorly understood.

4.1 The capuchin monkey has a complex primary motor cortex

The anatomy, electrophysiological properties and connectivity patterns of primate motor areas, especially those of Old World monkeys, have been extensively studied. The combination of Nissl, myelin and SMI-32 staining techniques, in

association with peripheral and cortical electrical stimulation techniques, allowed for the detailed mapping of motor areas, helping us understand the complexity of the motor cortex and its importance to the control of hand movements. A common finding of these studies is that the primary motor cortex is not uniform but composed of different subregions with distinct characteristics. In the owl monkey, the caudal part of the primary motor cortex has pyramidal cells larger than those of the rostral part, showing two subdivisions for this area: M1c (caudal) and M1r (rostral) (Stepniewska et al., 1993; Preuss et al., 1996). Preuss et al. (1997) described 3 subdivisions of the primary motor cortex based on SMI 32 immunostaining in *Macaca mulatta* and *M. nemestrin*: areas 4c, 4i and 4r, along the mediolateral axis. These data corroborate those of the present study, in which three subdivisions, F1c, F1i and F1r, are described in the primary motor cortex of the capuchin monkey. In all studies mentioned above, the main criteria for defining motor areas were the size, density, and distribution of Betz cells. These pyramidal cells are the largest neurons found in the entire cerebral cortex and represent a great proportion of the neurons that send projections to the motor neurons in spinal cord (Dum and Strick, 2005). Thus, the great density of these cells in the primary motor cortex reveals the importance of this area to the control of body movements, including those of the hands. Furthermore, studies based on electrical microstimulation, connectivity patterns and neuronal architecture provide concrete evidence to support partitioning of the primary motor cortex (Godschalk et al., 1995; Geyer et al., 1996; Dea et al., 2016; Hamadjida et al., 2016; Schellekens et al., 2018; Mayer et al., 2019).

The hand representation in the primary motor cortex extends across all its subdivisions. The movements evoked by intracortical microstimulation tend to be smaller when current is applied in the caudal part of M1, where the largest Betz cells are found. In the macaque, neurons in caudal M1 are also the ones projecting to the ventral horn of the spinal cord, which controls the muscles of the hands and arms (Rathelot and Strick, 2009). Therefore, representation of the hand in the primary motor cortex is part of an extensive network of cortical areas that interact to produce hand movements.

Many premotor and somatosensory areas project to the primary motor cortex (Dum and Strick, 2005). Neuroanatomical tracers' studies in New World monkeys show that the hand representations located in the caudal and rostral portion of M1 receive different inputs from somatosensory areas. Namely, projections are denser in the caudal as compared to the rostral portion of M1 (Dea et al., 2016). In squirrel monkeys, projections from the ventral premotor cortex mainly targets three subregions of M1: the rostro-medial (RM), the rostro-lateral (RL) and the caudo-lateral (CL) subregions. Only the caudo-medial region (CM) of M1 receives projections from ventral premotor areas (Stepniewska et al., 2006). This result supports the notion that functional parcellation of the primary motor cortex is not limited to its caudal-rostral axis. Additionally, it suggests that different segments of M1 are part of specific networks involved in unique aspects of manual behaviors (Dea et al., 2016; Mayer et al., 2019). This is in accordance with the fact that hand movements are markedly developed in the capuchin monkey. These animals perform precision movements with their fingers, such as

the pinch movement, in which the distal phalanx of the thumb touches the middle of the distal phalanx of any finger, regardless of the movement of the other fingers that do not touch the thumb (Christel and Fragaszy, 2000). Other New World Monkeys such as the squirrel monkey, spider monkey or the owl monkey are only able to perform object grasping by using all fingers flexed simultaneously towards the palm of the hand, regardless of the position of the thumb (Costello and Fragaszy, 1988). In these primates, the thumb movement corresponds to a pseudo position, meaning that it is unable to touch the ventral surface of the other digits (Cartmill, 1974).

In Old World monkeys such as macaques we find an opposable thumb engaged in a variety of manual behaviors and precision grips (Macfarlane and Graziano, 2009). Baldwin et al. (2018) described the details of elaborate digital movements evoked by electrical microstimulation of the motor or parietal cortex. Movements evoked by electric microstimulation of M1, as well as the motor map representations found in M1 of the capuchin monkey strongly resemble those found in the macaque in three important ways: 1) the primary motor cortex is dominated by the forelimb representation; 2) the representation of the hand is located at the level of the superior arcuate sulcus; and 3) many of the evoked hand movements, specifically those involving finger flexion, are similar between the two species (Macfarlane and Graziano, 2009). Thus, the organization of the capuchin monkey hand representation resembles much more the one described for the macaque than the representation described for any other New World primate (Gharbawie et al., 2010). In addition, as mentioned above, the architecture of the capuchin monkey primary motor cortex strongly resembles the one described for Old World monkeys, suggesting that similar selective pressures acted on both groups of animals (Kaas, 2012).

4.2 The capuchin monkey has a complex ventral premotor cortex (PMv)

Studies of macaque area PMv have led to two different points of view regarding its architectural organization. One view is that PMv consists of distinct cortical areas located at different dorsoventral levels of the brain. Vogt and Vogt (1919) subdivided this region into four architectural areas: area 4C, extending from the lower portion of the cs to the ias, and areas 6a α , 6b α and 6b β , ventral to 4C and marginal to ias. Areas 6a α and 6b α occupy different heights of the ias margin, while area 6b β is located at the final margin of ias. Barbas and Pandya (1987) proposed a similar subdivision based on cyto- and myeloarchitecture. According to them, PMv comprises area 4C, distinct from area 4, and two more ventral areas – 6Va and 6Vb – roughly corresponding to areas 6a α and 6b β of Vogt and Vogt (1919), respectively. Vogt's area 6b β was considered part of prefrontal area 12.

A dorso-ventral parcellation of PMv was also proposed by Preuss and Goldmann-Rakic (1991) based on myeloarchitectural criteria. Two areas were identified in their study: one dorsal and wider and one ventral and smaller, designated as areas 6Va and 6Vb, respectively. Area 6Va includes area 4C and 6Va as described

by [Barbas and Pandya \(1987\)](#). Area 6Vb appears overlapping with area 6Vb as described by [Barbas and Pandya \(1987\)](#).

The second view is that the architectural organization of PMv, as proposed by [von Bonin and Bailey \(1947\)](#) based on myeloarchitecture criteria, consists of distinct areas located at different rostro-caudal levels. Namely, two areas were located rostral to the area FA (corresponding to area 4): a more caudal one, designated as the FBA and a more rostral one, named as FCBm. A similar division was proposed by [Matelli et al. \(1985\)](#) using cytochrome oxidase histochemistry. Based on the laminar profile of enzymatic activity, they identified two distinct histochemical PMv areas: one caudal (F4) and one rostral (F5) corresponding to the FBA and FCBm areas of [von Bonin and Bailey \(1947\)](#), respectively.

Our present study supports this latter view. We subdivided the capuchin monkey PMv into areas F5p, F5c and F5a, which extend along the sas (spur) until the end of ias, and F4, which extends between the cs and the spur of the arcuate sulcus. Our data provide multi-architectural evidence for the rostro-caudal subdivision of this region into two areas, one more caudal (F4) and one more rostral (F5c) that seem to correspond to the cytoarchitectural areas FBA and FCBm of [von Bonin and Bailey \(1947\)](#), respectively. These two areas partially overlap with the cytoarchitectural subdivisions of [Vogt and Vogt \(1919\)](#) and [Barbas and Pandya \(1987\)](#). Specifically, F4 appears to correspond more dorsally to the rostral part of Vogt's area 4C and Barbas and Pandya's area 4C. The correspondence between our work and the studies mentioned above indicates a great degree of similarity between the motor areas of macaque and capuchin monkeys regarding PMv. However, the complex morphological characteristics of the motor areas impose challenges regarding their overlap and anatomical correspondence.

The subdivisions of PMv that we propose in this study are also in accordance with the pattern of cortico-cortical connectivity between posterior parietal and motor areas of the capuchin monkey. [Mayer et al. \(2016\)](#) showed that area F5 is interconnected with areas 5v, AIP, PFG and PF, which are areas of the posterior parietal cortex (PPC) intimately involved in controlling hand movement.

Among the areas of primate premotor cortex, F5 is critical for manual control, especially for object and tool manipulation, such as observed in the capuchin monkey. F5 is involved in the planning, execution, and coordination of complex hand movements. Additionally, it is reciprocally connected with area F1 and with areas of the parietal and prefrontal cortex ([Kurata, 2018](#)). In the present study, we subdivide area F5 into different regions, which is in accordance with the work by [Belmalih et al. \(2009\)](#). F5 is reciprocally connected (directly or indirectly) with the parietal ([Mayer et al., 2019](#)), frontal ([Luppino et al., 1993](#)), prefrontal ([Rizzolatti and Arbib, 1998](#)), temporal ([Rizzolatti and Luppino, 2001](#)) and areas of the cingulate and insular cortices ([Kurata, 2018](#)). Moreover, according to [Kurata \(2018\)](#), areas F5c and F5a are of higher hierarchical order within the ventral premotor cortex, since they are intimately interconnected with areas 44 and 12 of the dorsolateral prefrontal cortex, considered to be high-level association areas. Areas F5p and F4, the remaining areas in the ventral premotor cortex, are interconnected with areas AIP and VIP, respectively, which are responsible for processing visual,

visuomotor, and somatosensory fields. Therefore, according to [Caminiti et al. \(2017\)](#) the ventral premotor cortex can be subdivided into two large groups, with F5p and F4 more dorsal and F5a and F5c more ventral. Information first arrives in F5a and F5c and subsequently flows toward the more dorsal F4 and F5p areas. In other words, information flows from the rostroventral axis to the caudodorsal axis within PMv. Area F5p would be responsible for eye movements and for observed movements through the action of mirror neurons that respond to visual and auditory stimuli.

Areas F4 and F5p are associated with proximal and distal movements of the forelimbs. On the other hand, areas F5c and F5a are associated with decision-making processes based on somatosensory, auditory, and visual stimuli, in addition to short and long-term memory ([Gerbella et al., 2017](#)). The connectivity pattern of these regions with cortical areas 44 and 12 support these functions. Therefore, macaque area 44 would be homologous to human Broca's area, while macaque F5a would be homologous to human area 44. There is not enough data to support similar homologies in the capuchin monkey. However, it may be argued that the similarities in motor cortex organization between capuchin monkey and World Old monkeys are due to convergent evolution as a result of similar selective pressures acting on their motor function. If this is the case, the cytoarchitectural similarities between their motor areas evolved in parallel and independently across time.

4.3 Area PMd in capuchin monkeys

We were able to clearly differentiate the dorsal from the ventral motor areas in the capuchin monkey. Notably, we were able to subdivide the dorsal premotor cortex into areas F2 and F7. Based on the distribution and size of pyramidal cells, we were able to subdivide area F2 into dorsal (F2d) and ventral (F2v) portions, where pyramidal neurons were more abundant and larger in F2d. Our results are in apparent contradiction with the findings of [Geyer et al. \(2000\)](#), where they analyzed the distribution of neurofilament proteins in the dorsolateral premotor cortex of the macaque. They reported a stronger immunoreactivity and higher cell density in layer V of area F2v. This difference between species can be due to intraspecific phenotypic variation and to the fact that both areas represent different parts of the body: area F2d contains a representation of the leg while F2v contains a representation of the arm. However, the portions of F1 representing the leg versus arm do not exhibit any major difference between them ([Geyer et al., 2000](#)). It is thereby reasonable to speculate that variations in layer V between F2d and F2v are restricted to the pattern of fibers projecting from the cortex to the spinal cord and brainstem ([Dum and Strick, 2005](#)).

Numerous studies indicate that neurofilament proteins participate in the maintenance and stabilization of the axon cytoskeleton ([Morris and Lasek, 1982](#)). Its presence in the cell body has been correlated with neuron size and conduction velocity in the corresponding nerve fibers ([Hoffman et al., 1987](#)). For example, the relative amount of neurofilament proteins is low in short cortico-cortical connections, intermediate in non-callosal visual connections and high in association pathways and callosal

visual connections (Campbell et al., 1991; Hof et al., 1997). Probably, the observed difference in neurofilament distribution between areas F2d and F2v are due to the differential distribution of “slow” and “fast” pyramidal tract neurons. According to Verhaart (1948), 10% of the pyramidal tract fibers have axonal diameters that are approximately 3 micrometers wide (fast fibers). However, these giant pyramidal cells may contribute with only 3% of the descending fibers. At least 7% of fast fibers probably originate in large pyramidal neurons that are not classified as giant cells. SMI-32 immunopositivity in layer V may correspond to this fast fiber population. According to Evarts (1968), these neurons are mostly silent when the animal is at rest, but fire during movement. The presence of SMI-32 positive neurons in layer V of F2v may be due to the role of this area in the motor control of arm movements. The difference between F2d and F2v may also be related to the differential organization of descending projections. Area F2 projects to the reticular formation, where about 30% of this cortico-reticular projection sends collaterals to the spinal cord. Many F2v neurons project to both the reticular formation and to the spinal cord, while area F2d seems to project almost exclusively to the spinal cord (Keizer and Kuypers, 1989).

Raos et al. (Raos et al., 2003; Raos et al., 2004) demonstrated that within area F2 there is a distal anterior field that evokes finger movements. Some of these neurons selectively control the type of prehension movement necessary to grasp objects, indicating a key role of F2 in the control of skilled hand movements. Additionally, F2 neurons are also involved in motor learning, as they apparently hold in memory the representation of various hand movements. Based on visual information, F2 neurons are able to continuously update hand configuration and position in order to correctly grasp an object. Accordingly, F2 is required for the accuracy of grasping while the movement is in progress (Gomez et al., 2000). Area F7 plays a role in directing the eyes to the object of interest while visual information is necessary for recognizing the object.

The supplementary eye field (SEF) is situated inside area F7. The SEF is an oculomotor field that is richly interconnected with the frontal eye field (FEF) and that can be identified using intracortical micro-stimulation. The remaining portion of F7 seems to be poorly excitable using microstimulation and has thereby been the subject of a limited number of functional studies. Some of these F7 neurons have visual responses even when the stimulus is not instructing subsequent movement. Other F7 neurons exhibit visual responses when the location of the stimulus matches the target of an arm movement. Area F7 is not a source of corticospinal projections, but it is interconnected with areas F2 and F6. Parietal afferents are modest and originate mainly in PGm, an area located in the medial wall of the cerebral hemisphere. PGm is connected with PG and with extrinsic visual areas. In contrast to the weak parietal input, F7 is a target of strong projections from the dorsal part of the dorsolateral prefrontal cortex. Together, these results indicate that the regions that constitute dorsal area 6 are involved in different aspects of movement control. Area F2 seems to be involved in planning and executing arm and leg movements based on somatosensory and visual information. F7 seems to be involved in encoding object location in order to guide and coordinate body and arm movements. Another higher function of F7 (and dorsal area 6

in general) is suggested by lesion studies. Ablation of dorsal area 6 (i.e., areas F7 and F2) in monkeys trained to perform goal-directed movements in response to arbitrary external stimuli affects performance on previously learnt motor association tasks, while also hindering the learning of new tasks. It is thereby possible that dorsal area 6 is involved in motor control and in retrieving from memory the motor response most appropriate to the current behavioral context (Luppino and Rizzolatti, 2000).

4.4 Evolution of the motor cortex and manual skill

Kaas and collaborators proposed that the motor areas located in the frontal cortex underwent enlargement and subdivisions in early primates. Rodents and tree shrews represent the closest living groups to primates and thereby serve as good comparative models. Their primary and secondary motor areas probably correspond to the primate dorsal premotor cortex (Remple et al., 2007). In contrast, Galagos and anthropoid primates have an enlarged M1 area containing an expanded portion that represents movements of the forelimbs and digits. Galagos also have dorsal and ventral premotor areas, a frontal eye field (FEF), a supplementary motor area (SMA), and at least two motor regions in the cingulate cortex located at the medial border of the cerebral cortex. Therefore, as these motor areas are present in both Strepsirrhini and Haplorrhini monkeys, it is plausible that they evolved after Scandentia/Dermoptera and primates diverged from their common ancestor (Kaas, 2004; Kaas et al., 2008; Kaas, 2012). Such comparative studies also indicate that early primates had a region in the agranular frontal cortex with sensory input and connections with the dorsal and ventral premotor cortices, which in turn projected to M1. Many of these motor areas, together with the somatosensory areas, projected to interneurons and motor neurons in the spinal cord, but most of these projections were to M1 (Kaas, 2004). Goldring and Krubitzer (2017) argue that motor skills in primates evolved by the co-evolution of the hands and of the motor and posterior parietal areas that jointly control reaching, grasping and object exploration behavior. These capabilities are conspicuous in some New World primates such as capuchin monkeys of the genus *Cebus* and *Sapajus* (Lynch-Alfaro et al., 2012), in Old World monkeys of the genus *Macaca* (Malaivijitnond et al., 2007) and in large hominoid primates such as gorillas, chimpanzees, bonobos, orangutans, and humans (Seed and Byrne, 2010).

Regarding Brodmann's area 6 parceled out in our study, its ventral areas are already present in the earliest primates, such as galago and owl monkey. Both have a small PMv rostral to M1 (Kurata, 2018). On the other hand, PMd areas can be found in rodents and tree shrews (Kaas, 2012). Early primates had a certain ability to manipulate objects. However, more sophisticated manual skills appeared only later in primate evolution. Highly skilled hand movements eventually evolved in macaque and capuchin monkeys, chimpanzees, and humans (Wu et al., 2000). The ability to perform elaborate hand movements is also dependent on the size of the brain and the spinal cord, as well as on the number of sensorimotor fibers

coursing through the spinal cord. It is hypothesized that the enlargement of the brain and spinal cord resulted in an increased number of sensorimotor fibers capable of supporting manual dexterity and object manipulation skills (Rilling and Insel, 1999). At the cortical level, capuchin monkeys have the following characteristics that support skilled hand movements: 1) differentiated motor maps specifically representing the hand; 2) multiple premotor areas; 3) well-differentiated parietal areas associated with proprioception, and 4) the presence of area 5, which is associated with motor planning and visual guidance for reaching, grasping and object manipulation. The aforementioned areas communicate with area F5, which is also important for manual movements (Padberg et al., 2007). Furthermore, M1 neurons that project to the ventral premotor cortex, dorsal premotor cortex, supplementary motor area, or parietal area 5 are segregated in specific zones within the M1 hand representation. It has been suggested that this fine modular organization within the M1 hand representation can support parallel and simultaneous interactions with multiple specialized cortical areas in order to increase the complexity of hand movements (Hamadjida et al., 2016).

5 Conclusion

Here, we characterize the anatomical organization of the capuchin monkey motor cortex, where we describe 12 different cortical areas: F1c, F1i, F1r, F2d, F2v, F3, F4, F5a, F5c, F5p, F6 and F7. The capuchin monkey is unique among other New World primates for exhibiting highly skilled hand movements (Truppa et al., 2019). Our results also show that areas M1 and PM in the capuchin monkey exhibit a more complex organization compared to those of other New World monkeys with comparatively more limited manual motor skills. Notably, M1 and PMv are believed to interact in a decisive way during the planning, execution and control of fine hand and finger movements. The complexity of motor skills observed in the capuchin monkey is comparable to those of Old World monkeys, even though their last shared common ancestor dates back 40 million years ago. Curiously, we here report that the motor cortex of the capuchin monkey shares a high degree of similarity with the macaque monkey, an Old World primate. In addition to motor areas in the frontal cortex, parietal areas also show a high degree of similarity between New and Old World monkeys (Mayer et al., 2016; Mariani et al., 2019; Bonfim et al., 2023). Parallel convergent evolution is a possible explanation for the high degree of observed similarity between these groups. Namely, common evolutionary pressure requiring skilled hand use in both groups drove adaptations in both hand anatomy and in the corresponding spinal cord and brain architecture involved in motor control. However, it is still a speculative hypothesis and we do not know exactly the underlying processes involved.

Data availability statement

The raw data supporting the conclusions of this article will be made available by the authors, without undue reservation.

Ethics statement

The animal study was reviewed and approved by Ethics Committee for the Care and Use of Experimental Animals at the Center for Health Science, Federal University of Rio de Janeiro.

Author contributions

All authors have full access to all the data in the study and take responsibility for the integrity of the data and the accuracy of the data analysis. Study concept and design: EM-J, AO. Acquisition of data: EM-J, VB, MN-S, JS. Analysis and interpretation of data: EM-J, AM, JS. Preparation of illustrations: EM-J, RG. Critical revision of the article for important intellectual content: JS, RG, BL, MN-S, VB, EM-J, AM. Acquisition of funding: RG, JS. All authors contributed to the article and approved the submitted version.

Funding

This work was supported by the Fundação Carlos Chagas Filho de Amparo à Pesquisa do Estado do Rio de Janeiro (FAPERJ), Grant/Award Number: E-26/211.635/2021, E-26/201.357/2021, E-26/211.258/2019, E-26/110.905/2013, E-26/210.917/2016; Financiadora de Estudos e Projetos (FINEP), Grant/Award Number: PEC20150 (0354/16); Conselho Nacional de Desenvolvimento Científico e Tecnológico (CNPq), Grant/Award Number: 471.166/2013-8. EGM was awarded a scholarship from the Brazilian CAPES funding agency.

Acknowledgments

This study is part of the Master Dissertation of EM-J, who was affiliated with the Graduate Program in Biological Sciences – Physiology at the Federal University of Rio de Janeiro (UFRJ, <https://www.posgraduacao.biof.ufrj.br/en>). This paper was done under the supervision of Professor João Guedes da Franca. His contribution to this paper was fundamental. Unfortunately, João Franca passed away before this manuscript was finished and was thereby not able to approve its final version. That is the sole reason Prof. Franca is not listed as an author.

Conflict of interest

The authors declare that the research was conducted in the absence of any commercial or financial relationships that could be construed as a potential conflict of interest.

The author JS declared that they were an editorial board member of Frontiers, at the time of submission. This had no impact on the peer review process and the final decision.

References

- Baldwin, M. K. L., Cooke, D. F., Goldring, A. B., and Krubitzer, L. (2018). Representations of fine digit movements in posterior and anterior parietal cortex revealed using long-train intracortical microstimulation in macaque monkeys. *Cereb. Cortex* 28, 4244–4263. doi: 10.1093/cercor/bhx279
- Barbas, H., and Pandya, D. N. (1987). Architecture and frontal cortical connections of the premotor cortex (area 6) in the rhesus monkey. *J. Comp. Neurol.* 256, 211–228. doi: 10.1002/cne.902560203
- Barbas, H., and Pandya, D. N. (1989). Architecture and intrinsic connections of the prefrontal cortex in the rhesus monkey. *J. Comp. Neurol.* 286, 353–375. doi: 10.1002/cne.902860306
- Belmalih, A., Borra, E., Contini, M., Gerbella, M., Rozzi, S., and Luppino, G. (2009). Multimodal architectonic subdivision of the rostral part (Area F5) of the macaque ventral premotor cortex. *J. Comp. Neurol.* 512, 183–217. doi: 10.1002/cne.21892
- Bezgin, G., Vakorin, V. A., van Opstal, A. J., Mcinstosh, A. R., and Bakker, R. (2012). Hundreds of brain maps in one atlas: registering coordinate-independent primate neuro-anatomical data to a standard brain. *NeuroImage* 62, 67–76. doi: 10.1016/j.neuroimage.2012.04.013
- Bonfim, V., Mayer, A., Nascimento-Silva, M. L., Lima, B., Soares, J. G. M., and Gattass, R. (2023). Architecture of the inferior parietal cortex in capuchin monkey. *J. Comp. Neurol.* 2023, 1–17. doi: 10.1002/cne.25449
- Brodman, K. (1905). Beiträge zur histologischen lokalisation der grosshirnrinde. dritte mitteilung: die rindenfelder der niederen affen. *J. Psychol. Neurol. Lpz* 4, 177–226.
- Caminiti, R., Borra, E., Visco-Comandini, F., Battaglia-Mayer, A., Averbeck, B. B., and Luppino, G. (2017). Computational architecture of the parieto-frontal network underlying cognitive-motor control in monkeys. *eNeuro* 4:ENEURO.0306-16.2017. doi: 10.1523/ENEURO.0306-16.2017
- Caminiti, R., Innocenti, G. M., and Battaglia-Mayer, A. (2015). Organization and evolution of parieto-frontal processing streams in macaque monkeys and humans. *Neurosci. Biobehav. Rev.* 56, 73–96. doi: 10.1016/j.neubiorev.2015.06.014
- Campbell, A. W. (1904). Histological studies on the localization of cerebral function. *J. Ment. Sci.* 50, 651–62. doi: 10.1192/bjp.50.211.651
- Campbell, M. J., Hof, P. R., and Morrison, J. H. (1991). A subpopulation of primate corticocortical neurons is distinguished by somatodendritic distribution of neurofilament protein. *Brain Res.* 539, 133–136. doi: 10.1016/0006-8993(91)90695-R
- Campbell, M. J., and Morrison, J. H. (1989). Monoclonal antibody to neurofilament protein (SMI-32) labels a subpopulation of pyramidal neurons in the human and monkey neocortex. *J. Comp. Neurol.* 282, 191–205. doi: 10.1002/cne.902820204
- Cartmill, M. (1974). Rethinking primate origins the characteristic primate traits cannot be explained simply as adaptations to arboreal life. *Science* 184, 436–443. doi: 10.1126/science.184.4135.436
- Chaplin, T. A., Hsin-Hao, Y., Soares, J. G. M., Gattass, R., and Rosa, M. G. P. (2013). A conserved pattern of differential expansion of cortical areas in simian primates. *J. Neurosci.* 33, 15120–15125. doi: 10.1523/JNEUROSCI.2909-13.2013
- Christel, M., and Frigaszy, D. M. (2000). Manual function in *Cebus apella*. digital mobility, reshaping, and endurance in repetitive grasping. *Int. J. Primatol.* 21, 697–719. doi: 10.1023/A:1005521522418
- Costello, M. B., and Frigaszy, D. M. (1988). Prehension in *Cebus* and *Saimiri*: grip type and hand preference. *Am. J. Primatol.* 15, 235–245. doi: 10.1002/ajp.1350150306
- Dea, M., Hamadjida, A., Elgebeili, G., Quessy, S., and Dancause, N. (2016). Different patterns of cortical inputs to subregions of the primary motor cortex hand representation in *Cebus apella*. *Cereb. Cortex* 26, 1747–1761. doi: 10.1093/cercor/bhv324
- Dum, R. P., and Strick, P. L. (1991). The origin of corticospinal projections from the premotor areas in the frontal lobe. *J. Neurosci.* 11, 667–689. doi: 10.1523/JNEUROSCI.11-03-00667.1991
- Dum, R. P., and Strick, P. L. (2005). Frontal lobe inputs to the digit representations of the motor areas on the lateral surface of the hemisphere. *J. Neurosci.* 25, 1375–1386. doi: 10.1523/JNEUROSCI.3902-04.2005
- Evarts, E. V. (1968). A technique for recording activity of subcortical neurons in moving animals. *Electroenceph. Clin. Neurophysiol.* 24, 83–86. doi: 10.1016/0013-4694(68)90070-9
- Fiorani, M. Jr, Gattass, R., Rosa, M. G. P., and Sousa, A. P. (1989). Visual area MT in the *Cebus* monkey: location, visuotopic organization, and variability. *J. Comp. Neurol.* 287, 98–118. doi: 10.1002/cne.902870108
- Fragaszy, D. (1983). Preliminary quantitative studies of prehension in squirrel monkeys (*Saimiri sciureus*). *Brain Behav. Evol.* 23, 81–92. doi: 10.1159/000121499
- Gabernet, L., Meskenaite, V., and Hepp-Reymond, M. C. (1999). Parcellation of the lateral premotor cortex of the macaque monkey based on staining with the neurofilament antibody SMI-32. *Exp. Brain Res.* 128, 188–193. doi: 10.1007/s002210050834
- Gallyas, F. (1979). Silver staining of myelin by means of physical development. *Neurol. Res.* 1, 203–209. doi: 10.1080/01616412.1979.11739553
- Gattass, R., Sousa, A. P. B., and Rosa, M. G. P. (1987). Visual topography of V1 in the *Cebus* monkey. *J. Comp. Neurol.* 259, 529–548. doi: 10.1002/cne.902590404
- Gerbella, M., Rozzi, S., and Rizzolatti, G. (2017). The extended object-grasping network. *Exp. Brain Res.* 235, 2903–2916. doi: 10.1007/s00221-017-5007-3
- Geyer, S. (2004). The microstructural border between the motor and the cognitive domain in the human cerebral cortex. *Adv. Anat. Embryol. Cell Biol.* 174, 1–89. doi: 10.1007/978-3-642-18910-4
- Geyer, S., Ledberg, A., Schleicher, A., Kinomura, S., Schormann, T., Bürgel, U., et al. (1996). Two different areas within the primary motor cortex of man. *Nature* 382, 805–807. doi: 10.1038/382805a0
- Geyer, S., Zilles, K., Luppino, G., and Matelli, M. (2000). Neurofilament protein distribution in the macaque monkey dorsolateral premotor cortex. *Eur. J. Neurosci.* 12, 1554–1566. doi: 10.1046/j.1460-9568.2000.00042.x
- Gharbawie, O. A., Stepniewska, I., Burish, M. J., and Kaas, J. H. (2010). Thalamocortical connections of functional zones in posterior parietal cortex and frontal cortex motor regions in new world monkeys. *Cereb. Cortex* 20, 2391–2410. doi: 10.1093/cercor/bhp308
- Godschalk, M., Mitz, A. R., Van Duijn, B., and van der Burg, H. (1995). Somatotopy of monkey premotor cortex examined with microstimulation. *Neurosci. Res.* 23, 269–279. doi: 10.1016/0168-0102(95)00950-7
- Goldring, A., and Krubitzer, L. (2017). “Evolution of parietal cortex in mammals: from manipulation to tool use,” in *The evolution of nervous systems*. Eds. L. Krubitzer and J. H. Kaas (London: Elsevier), 259–286.
- Gomez, J. E., Fu, Q., Flament, D., and Ebner, T. J. (2000). Representation of accuracy in the dorsal premotor cortex. *Eur. J. Neurosci.* 12, 3748–3760. doi: 10.1046/j.1460-9568.2000.00232.x
- Hamadjida, A., Dea, M., Deffeyes, J., Quessy, S., and Dancause, N. (2016). Parallel cortical networks formed by modular organization of primary motor cortex outputs. *Curr. Biol.* 26, 1737–1743. doi: 10.1016/j.cub.2016.04.068
- Hof, P. R., and Morrison, J. H. (1995). Neurofilament protein defines regional patterns of cortical organization in the macaque monkey visual system - a quantitative immunohistochemical analysis. *J. Comp. Neurol.* 352, 161–186. doi: 10.1002/cne.903520202
- Hof, P. R., Vogt, B. A., Bouras, C., and Morrison, J. H. (1997). Atypical form of alzheimer's disease with prominent posterior cortical atrophy: a review of lesion distribution and circuit disconnection in cortical visual pathways. *Vision Res.* 37, 3609–3625. doi: 10.1016/S0042-6989(96)00240-4
- Hoffman, E. P., Brown, R. H., and Kunkel, L. M. (1987). Dystrophin: the protein product of the duchenne muscular dystrophy locus. *Cell* 51, 919–928. doi: 10.1016/0092-8674(87)90579-4
- Kaas, J. H. (2004). Evolution of somatosensory and motor cortex in primates. *anat. rec. a discov. Mol. Cell Evol. Biol.* 281, 1148–1156. doi: 10.1002/ar.a.20120
- Kaas, J. H. (2012). The evolution of neocortex in primates. *Prog. Brain Res.* 195, 91–102. doi: 10.1016/B978-0-444-53860-4.00005-2

Publisher's note

All claims expressed in this article are solely those of the authors and do not necessarily represent those of their affiliated organizations, or those of the publisher, the editors and the reviewers. Any product that may be evaluated in this article, or claim that may be made by its manufacturer, is not guaranteed or endorsed by the publisher.

- Kaas, J. H., Qi, H. X., Burish, M. J., Gharbawie, O. A., Onifer, S. M., and Massey, J. M. (2008). Cortical and subcortical plasticity in the brains of humans, primates, and rats after damage to sensory afferents in the dorsal columns of the spinal cord. *Exp. Neurol.* 209, 407–416. doi: 10.1016/j.expneurol.2007.06.014
- Kalwani, R. M., Bloy, L., Elliott, M. A., and Gold, J. I. (2009). A method for localizing microelectrode trajectories in the macaque brain using MRI. *J. Neurosci. Methods* 176, 104–111. doi: 10.1016/j.jneumeth.2008.08.034
- Kantak, S. S., Mummidisetty, C. K., and Stinear, J. W. (2012). Primary motor and premotor cortex in implicit sequence learning – evidence for competition between implicit and explicit human motor memory systems. *Eur. J. Neurosci.* 36, 2710–2715. doi: 10.1111/j.1460-9568.2012.08175.x
- Keizer, K., and Kuypers, H. (1989). Distribution of corticospinal neurons with collaterals to the lower brain stem nuclei reticular formation in monkey (*Macaca fascicularis*). *Exp. Brain Res.* 74, 311–318. doi: 10.1007/BF00248864
- Kurata, K. (2018). Hierarchical organization within the ventral premotor cortex of the macaque monkey. *Neuroscience* 382, 127–143. doi: 10.1016/j.neuroscience.2018.04.033
- Luppino, G., Matelli, M., Camarda, R., Gallese, V., and Rizzolatti, G. (1991). Multiple representations of body movements in mesial area 6 and the adjacent cingulate cortex: an intracortical microstimulation study. *J. Comp. Neurol.* 311, 463–482. doi: 10.1002/cne.903110403
- Luppino, G., Matelli, M., Camarda, R., and Rizzolatti, G. (1993). Corticocortical connections of area F3 (SMA-proper) and area F6 (pre-SMA) in the macaque monkey. *J. Comp. Neurol.* 338, 114–140. doi: 10.1002/cne.903380109
- Luppino, G., and Rizzolatti, G. (2000). The organization of the frontal motor cortex. *Physiology* 15, 219–224. doi: 10.1152/physiologyonline.2000.15.5.219
- Lynch-Alfaro, J. W., De Souza e Silva, J., and Rylands, A. B. (2012). How different are robust and gracile capuchin monkeys? an argument for the use of *Sapajus* and *Cebus*. *Am. J. Primatol.* 74, 273–286. doi: 10.1002/ajp.22007
- Macfarlane, N. B. V., and Graziano, M. S. A. (2009). Diversity of grip in *Macaca mulatta*. *exp. Brain Res.* 197, 255–268. doi: 10.1007/s00221-009-1909-z
- Malaivijitnond, S., Lekprayoon, C., Tandavanittj, N., Panha, S., Cheewatham, C., and Hamada, Y. (2007). Stone-tool usage by Thai long-tailed macaques (*Macaca fascicularis*). *Am. J. Primatol.* 69, 227–233. doi: 10.1002/ajp.20342
- Mannu, M., and Ottoni, E. B. (2009). The enhanced tool-kit of two groups of wild bearded capuchin monkeys in the caatinga: tool making, associative use, and secondary tools. *Am. J. Primatol.* 71, 242–251. doi: 10.1002/ajp.20642
- Mariani, O. S. C., Lima, B., Soares, J. G. M., Mayer, A., Franca, J. G., and Gattass, R. (2019). Partitioning of the primate intraparietal cortex based on connectivity pattern and immunohistochemistry for cat-301 and SMI-32. *J. Comp. Neurol.* 527, 694–717. doi: 10.1002/cne.24438
- Matelli, M., Luppino, G., and Rizzolatti, G. (1985). Patterns of cytochrome oxidase activity in the frontal agranular cortex of macaque monkeys. *Behav. Brain Res.* 18, 125–136. doi: 10.1016/0166-4328(85)90068-3
- Matelli, M., Luppino, G., and Rizzolatti, G. (1991). Architecture of superior and mesial area 6 and the adjacent cingulate cortex in the macaque monkey. *J. Comp. Neurol.* 311, 445–462. doi: 10.1002/cne.903110402
- Matsuzaka, Y., Aizawa, H., and Tanji, J. (1992). A motor area rostral to the supplementary motor area (presupplementary motor area) in the monkey: neuronal activity during a learned motor task. *J. Neurophysiol.* 68, 653–662. doi: 10.1152/jn.1992.68.3.653
- Mayer, A., Baldwin, M. K. L., Cooke, D. F., Lima, B. R., Padberg, J., Lewenfus, G., et al. (2019). The multiple representations of complex digit movements in primary motor cortex form the building blocks for complex grip types in capuchin monkeys. *J. Neurosci.* 39, 6684–6695. doi: 10.1523/JNEUROSCI.0556-19.2019
- Mayer, A., Nascimento-Silva, M. L., Keher, N. B., Bittencourt-Navarrete, R. E., Gattass, R., and Franca, J. G. (2016). Architectonic mapping of somatosensory areas involved in skilled forelimb movements and tool use. *J. Comp. Neurol.* 524, 1399–1423. doi: 10.1002/cne.23916
- Morris, J. R., and Lasek, R. J. (1982). Stable polymers of the axonal cytoskeleton: the axoplasmic ghost. *J. Cell Biol.* 92, 192–198. doi: 10.1093/cercor/bhz051
- Moura, A., and Lee, P. (2004). Capuchin stone tool use in caatinga dry forest. *Science* 306, 1909. doi: 10.1126/science.1102558
- Padberg, J., Franca, J. G., Cooke, D. F., Soares, J. G. M., Rosa, M. G. P., Fiorani, J., et al. (2007). Parallel evolution of cortical areas involved in skilled hand use. *J. Neurosci.* 27, 10106–10115. doi: 10.1523/JNEUROSCI.2632-07.2007
- Passarelli, L., Gamberini, M., and Fattori, P. (2021). The superior parietal lobule of primates: a sensory-motor hub for interaction with the environment. *J. Integr. Neurosci.* 20, 157–171. doi: 10.31083/jjin.2021.01.334
- Penfield, W., and Boldrey, E. (1937). Somatic motor and sensory representation in the cerebral cortex of man as studied by electrical stimulation. *Brain* 60, 389–443. doi: 10.1093/brain/60.4.389
- Preuss, T. M., and Goldman-Rakic, P. S. (1991). Myelo- and cytoarchitecture of the granular frontal cortex and surrounding regions in the strepsirhine primate galago and the anthropoid primate *Macaca*. *J. Comp. Neurol.* 310, 429–474. doi: 10.1002/cne.903100402
- Preuss, T. M., Stepniewska, I., Jain, N., and Kaas, J. H. (1997). Multiple divisions of macaque precentral motor cortex identified with neuro-filament antibody SMI-32. *Brain Res.* 767, 148–153. doi: 10.1016/S0006-8993(97)00704-X
- Preuss, T. M., Stepniewska, I., and Kaas, J. H. (1996). Movement representation in the dorsal and ventral premotor areas of owl monkeys: a microstimulation study. *J. Comp. Neurol.* 371, 649–676. doi: 10.1002/(SICI)1096-9861(19960805)371:4<649::AID-CNE12>3.0.CO;2-E
- Raos, V., Franchi, G., Gallese, V., and Fofassi, L. (2003). Somatotopic organization of the lateral part of area F2 (dorsal premotor cortex) of the macaque monkey. *J. Neurophysiol.* 89, 1503–1518. doi: 10.1152/jn.00661.2002
- Raos, V., Umiltà, M. A., Gallese, V., and Fogassi, L. (2004). Functional properties of grasping-related neurons in the dorsal premotor area F2 of the macaque monkey. *J. Neurophysiol.* 92, 1990–2002. doi: 10.1152/jn.00154.2004
- Rathelot, J. A., and Strick, P. L. (2009). Subdivisions of primary motor cortex based on cortico-motoneuronal cells. *Proc. Natl. Acad. Sci. U.S.A.* 106, 918–923. doi: 10.1073/pnas.0808362106
- Remple, M. S., Reed, J. L., Stepniewska, I., Lyon, D. C., and Kaas, J. H. (2007). The organization of frontoparietal cortex in the tree shrew (*Tupaia belangeri*): II. connective evidence for a frontal-posterior parietal network. *J. Comp. Neurol.* 501, 121–149. doi: 10.1002/cne.21226
- Reser, D. H., Richardson, K. E., Montibeller, M. O., Zhao, S., Chan, J. M., Soares, J. G., et al. (2014). Claustrum projections to prefrontal cortex in the capuchin monkey (*Cebus apella*). *Front. Syst. Neurosci.* 8. doi: 10.3389/fnsys.2014.00123
- Rilling, J. K., and Insel, T. R. (1999). The primate neocortex in comparative perspective using magnetic resonance imaging. *J. Hum. Evol.* 37, 191–223. doi: 10.1006/jhev.1999.0313
- Rizzolatti, G., and Arbib, M. A. (1998). Language within our grasp. *Trends Neurosci.* 21, 188–194. doi: 10.1016/S0166-2236(98)01260-0
- Rizzolatti, G., Fogassi, L., and Gallese, V. (1997). Parietal cortex: from sight to action. *Curr. Opin. Neurobiol.* 7, 562–567. doi: 10.1016/S0959-4388(97)80037-2
- Rizzolatti, G., Gentilucci, M., Camarda, R., Gallese, V., Luppino, G., Matelli, M., et al. (1990). Neurons related to reaching-grasping arm movements in the rostral part of area 6 (area 6af5). *Exp. Brain Res.* 82, 337–350. doi: 10.1007/BF00231253
- Rizzolatti, G., and Luppino, G. (2001). The cortical motor system. *Neuron* 31, 889–901. doi: 10.1016/S0896-6273(01)00423-8
- Rizzolatti, G., Luppino, G., and Matelli, M. (1998). The organization of the cortical motor system: new concepts. *Electroencephalogr. Clin. Neurophysiol.* 106, 283–296. doi: 10.1016/S0013-4694(98)00022-4
- Rosa, M. G. P., Soares, J. G. M., Fiorani, M. J., and Gattass, R. (1993). Cortical afferents of visual area MT in the *Cebus* monkey: possible homologies between new and old world monkeys. *Vis. Neurosci.* 10, 827–855. doi: 10.1017/S095252380006064
- Schellekens, W., Petridou, N., and Ramsey, N. F. (2018). Detail somatopy in primary motor and somatosensory cortex revealed by Gaussian population receptive fields. *NeuroImage* 179, 337–347. doi: 10.1016/j.neuroimage.2018.06.062
- Seed, A. M., and Byrne, R. W. (2010). Animal tool use. *Curr. Biol.* 20, R1032–R1039. doi: 10.1016/j.cub.2010.09.042
- Spinozzi, G., Lubrano, G., and Truppa, V. (2004). Categorization of above and below spatial relations by tufted capuchin monkeys (*Cebus apella*). *J. Comp. Psychol.* 118, 403–412. doi: 10.1037/0735-7036.118.4.403
- Stepniewska, I., Preuss, T. M., and Kaas, J. H. (1993). Architectonics, somatotopic organization, and ipsilateral cortical connections of the primary motor area (M1) of owl monkeys. *J. Comp. Neurol.* 330, 238–271. doi: 10.1002/cne.903300207
- Stepniewska, I., Preuss, T. M., and Kaas, J. H. (2006). Ipsilateral cortical connections of dorsal and ventral premotor areas in new world owl monkeys. *J. Comp. Neurol.* 495, 691–708. doi: 10.1002/cne.20906
- Sternberger, L. A., and Sternberger, N. H. (1983). Monoclonal antibodies distinguish phosphorylated and nonphosphorylated forms of neurofilaments in situ. *Proc. Natl. Acad. Sci.* 80, 6126–6130. doi: 10.1073/pnas.80.19.6126
- Strick, P. L., and Preston, J. B. (1978). Sorting of somatosensory afferent information in primate motor cortex. *Brain Res.* 156, 364–368. doi: 10.1016/0006-8993(78)90520-6
- Tanji, J. (2001). Sequential organization of multiple movements: involvement of cortical motor areas. *Annu. Rev. Neurosci.* 24, 631–651. doi: 10.1146/annurev.neuro.24.1.631
- Truppa, V., Carducci, P., and Sabbatini, G. (2019). Object grasping and manipulation in capuchin monkeys (genera *Cebus* and *Sapajus*). *Biol. J. Linn. Soc.* 127, 563–582. doi: 10.1093/biolinnean/bly131
- Van Essen, D. C. (2005). A population-average, landmark-and surface-based (PALS) atlas of human cerebral cortex. *NeuroImage* 28, 635–662. doi: 10.1016/j.neuroimage.2005.06.058
- Van Essen, D. C. (2012). Cortical cartography and caret software. *NeuroImage* 62, 757–764. doi: 10.1016/j.neuroimage.2011.10.077
- Van Essen, D. C., Drury, H. A., Dickson, J., Harwell, J., Hanlon, D., and Anderson, C. H. (2001). An integrated software suite for surface-based analyses of cerebral cortex. *J. Am. Med. Assoc. Inform. Assoc.* 8, 443–459. doi: 10.1136/jamia.2001.0080443
- Verhaart, W. J. (1948). The pes pedunculii and pyramid. *J. Comp. Neurol.* 88, 139–156. doi: 10.1002/cne.900880106
- Vogt, C., and Vogt, A. (1919). Allgemeinere ergebnisse unserer hirnforchung. *J. Psychol. Neurol.* 25, 279–461.

- von Bonin, G., and Bailey, P. (1947). *The neocortex of macaca mulatta* (Urbana, IL: University of Illinois Press).
- Von Economo, C. (1929). Wie sollen wir elitegehirne verarbeiten? *Z Gesamte Neurol. Psychiatr.* 121, 323–409.
- Watanabe-Sawaguchi, K., Kubota, K., and Arikuni, T. (1991). Cytoarchitecture and intrafrontal connections of the frontal cortex of the brain of the hamadryas baboon (*Papio hamadryas*). *J. Comp. Neurol.* 311, 108–133. doi: 10.1002/cne.903110109
- Woolsey, C. N., Settlage, P. H., Meyer, D. R., Sencer, W., Pinto Hamuy, T., and Travis, A. M. (1952). Patterns of localization in precentral and "supplementary" motor areas and their relation to the concept of a premotor area. *Res. Publ. Assoc. Res. Nerv. Ment. Dis.* 30, 238–264.
- Wu, C. W. H., Bichot, N. P., and Kaas, J. H. (2000). Converging evidence from microstimulation, architecture, and connections for multiple motor areas in the frontal and cingulate cortex of prosimian primates. *J. Comp. Neurol.* 423, 140–177. doi: 10.1002/1096-9861(20000717)423:1<140::AID-CNE12>3.0.CO;2-3
- Zhong, J., Phua, D. Y. L., and Qiu, A. (2010). Quantitative evaluation of LDDMM, FreeSurfer, and CARET for cortical surface mapping. *Neuroimage* 52, 131–141. doi: 10.1016/j.neuroimage.2010.03.085